



Strål
säkerhets
myndigheten

Swedish Radiation Safety Authority

Research

Weld residual stress and strain measurements on a mock-up with single layer strip cladding common in reactor pressure vessels

2022:14

Authors: Daniel Mångård, Jens Gunnars,
Kiwa Technical Consulting AB, Solna

Report number: 2022:14

ISSN: 2000-0456

Available at: www.ssm.se

SSM perspektiv

Bakgrund

Reaktortryckkärl tillverkas vanligtvis av låglegerade ferritiska stål som på insidan beläggs med ett eller flera lager av rostfritt stål, så kallad plätering eller på engelska cladding. Den rostfria pläteringens påverkar den strukturella integriteten på flera sätt, dels har pläteringens annorlunda materialegenskaper jämfört med grundmaterialet vad gäller fysikaliska och mekaniska egenskaper, dels förbättrar pläteringens motståndet mot korrosion. Eftersom pläteringens materialegenskaper skiljer sig från de hos grundmaterialet uppstår i kallt tillstånd relativt stora svetsegensspänningar av dragkaraktär i pläteringsskiktet. Dessa omständigheter gör att pläteringens måste tas hänsyn till när man gör analyser av sprickor i närheten av pläteringens i ett reaktortryckkärl.

Svetsegensspänningar står normalt för stor del av spänningsbidraget vid utvärdering av reaktortryckkärls säkerhetsmarginaler. God kunskap om och goda uppskattningar av svetsegensspänningarna är därför viktigt vid olika typer av analyser, exempelvis vid analyser av fortsatt drift med skadad anordning eller analyser av långtidsdrift (LTO). I det senare fallet är goda uppskattningar särskilt viktiga vid analys av så kallade kalla lastfall för reaktortryckkärl, där brottsegheten i härdområdet minskat på grund av bestrålningsförsprödning.

Numeriska metoder kan användas för att bestämma svetsegensspänningar i mekaniska anordningar. För att dessa metoder ska vara pålitliga krävs normalt att de valideras mot verkliga fall eller noggrant uppmätta experiment. Föreliggande rapport beskriver ett experimentellt program, där bland annat spänningar, töjningar och temperaturer vid svetsning uppmättes för en plåt av reaktortryckkärlsmaterial som belagts med rostfri plätering.

Resultat

Svetsegensspänningarna hos den svetsade plåten uppmättes med ett antal olika tekniker och utfördes i olika positioner både före och efter värmebehandling. Resultaten från mätningarna visade på dragspänningar i nivå med sträckgränsen i pläteringens och cirka 30 mm in i grundmaterialet. Efter värmebehandling konstaterades kraftigt reducerade spänningar i grundmaterialet medan spänningarna i pläteringens var i princip oförändrade.

Resultaten är överensstämmande med de spänningsprofiler som erhållits i tidigare likande arbeten. De skillnader som noteras beträffar storleken av svetsegensspänningen och kan härledas till utformningen av experimentet, exempelvis geometri, randvillkor, svetsmetod, material och mätmetoder.

Relevans

Det genomförda projektet har förbättrat förståelsen kring svetsegensspänningars storlek och fördelning i området mellan plätering och grundmaterial i ett reaktortryckkärl. Vidare är resultaten

från projektet viktiga för att kunna validera numeriska metoder för bestämning av sådana svetsgenspänningar.

Behov av fortsatt forskning

Resultat och kunskaper från det genomförda projektet är viktiga för valideringen av numeriska metoder för att bestämma tillförlitliga svetsgenspänningar i området mellan plätering och grundmaterial. Arbetet med att ta fram och validera sådana numeriska metoder redovisas i forskningsprojektet SSM2015-924. Resultat och kunskaper från detta projekt och det aktuella är också användbara i ett pågående internationellt projekt kring analyser av reaktortryckkärlet. Detta projekt kallas APAL (*Advanced Pressurized Thermal Shock Analysis for LTO*) och redovisas i SSM2020-5721.

Projekt information

Kontaktperson SSM: Fredrik Forsberg

Referens: SSM2016-582-12 / 7030038-00



Strål
säkerhets
myndigheten

Swedish Radiation Safety Authority

Authors: Daniel Mångård, Jens Gunnars
Kiwa Technical Consulting AB, Solna

2022:14

Weld residual stress and strain measurements on a mock-up with single layer strip cladding common in reactor pressure vessels

Date: October 2022

Report number: 2022:14

ISSN: 2000-0456

Available at www.stralsakerhetsmyndigheten.se

This report concerns a study which has been conducted for the Swedish Radiation Safety Authority, SSM. The conclusions and viewpoints presented in the report are those of the author/authors and do not necessarily coincide with those of the SSM.

Authors

Daniel Mångård and Jens Gunnars

Title

Weld residual stress and strain measurements on a mock-up with single layer strip cladding common in reactor pressure vessels

Summary

Residual stress and strain measurements were performed on a mock-up consisting of a 160 mm thick low-alloy ferritic steel plate of type SA-508 Class 3 with a single layer weld deposited strip cladding of austenitic stainless steel E308L. The cladding was manufactured with submerged arc strip welding adapted to a procedure used for reactor pressure vessels in the 1970s. Comprehensive measurements of the thermal response during welding was recorded to provide information e.g. for validation of numerical modelling. Detailed through-thickness measurements of residual stresses were performed using the methods deep hole drilling and incremental centre-hole drilling, at two different locations in the as-welded state and at three different locations after post weld heat treatment.

The measurements show that high tensile residual stresses are found in the clad material and about 30 mm into the low-alloy ferritic steel after welding. The residual stresses in the clad layer and in the steel plate are in the order of the yield stress in each material. Further, measurements after post weld heat treatment show that the residual stresses in the low-alloy ferritic base material and butt weld were substantially reduced, whereas no significant reduction was observed for the residual stresses in the stainless steel cladding.

Neutron embrittlement of the reactor pressure vessel generally limits the possible long-term operation of a nuclear power plant to e.g. 60 or 80 years. Sufficient remaining safety margins with respect to fracture has to be verified by structural integrity analyses that consider the plant surveillance tests results, defects in and near the cladding, the dimensioning load cases, and also residual stresses in the reactor pressure vessel. For these reasons good understanding and well documented estimates of the residual stresses in the cladding are very valuable.

The residual stresses measured in the mock-up deviates from the residual stresses in a cladded reactor pressure vessel, since the mock-up was not subjected to pressure test. However, the detailed results presented in this report are very valuable for validation of numerical modelling, which can be used to predict the residual stress state including effects of pressure tests and operational loads, for cylindrical geometries, and for cladding processes other than submerged arc strip welding.

Contents

1.	INTRODUCTION	3
2.	MOCK-UP DESIGN	6
2.1	Base metal and weld overlay cladding	6
2.2	Submerged arc strip cladding	9
3.	OVERLAY WELDING	11
3.1	Welding parameters	11
3.2	Preheat and interpass temperatures	11
3.3	Post weld heat treatment	11
4.	TEMPERATURE MEASUREMENTS	13
5.	RESIDUAL STRESS MEASUREMENT TECHNIQUES	18
5.1	Deep hole drilling	18
5.2	Incremental centre-hole drilling	18
5.3	Ring coring	19
6.	RESIDUAL STRESS MEASUREMENT LOCATIONS	21
7.	RESIDUAL STRESS MEASUREMENT RESULTS	25
7.1	Cladded block in as-welded state	25
7.1.1	Location #3A - mid-strip, as-welded	25
7.1.2	Location #3B - mid-overlap, as-welded	26
7.2	Cladded block in post-weld heat treated state	27
7.2.1	Location #7A - mid-strip, after PWHT	27
7.2.2	Location #7B - mid-overlap, after PWHT	27
7.2.3	Location #5A - mid-strip, at butt weld, after PWHT	28
8.	DISCUSSION	34
9.	CONCLUSIONS	39
10.	CONTRIBUTION STATEMENT	42
11.	ACKNOWLEDGEMENT	42
12.	REFERENCES	43

1. Introduction

Pressure vessels fabricated from low-alloy ferritic steel are frequently internally protected from environmental effects by use of corrosion resistant materials. A protective cladding can be accomplished by depositing an austenitic stainless-steel weld overlay to the internal surfaces. Within the nuclear industry, one frequently adopted method during the 1970s to protect interior surfaces of reactor pressure vessels (RPV) was submerged arc strip cladding. This process is associated with high quality, high deposition rate and low dilution [1]. Other commonly used techniques to clad RPVs were series arc welding with three wires and manual arc welding.

The result from the cladding process is a protective layer that has chemical, thermal and mechanical material properties different to those of the base material [2]. These characteristics create the protective barrier but will also induce residual stresses which influence the structural integrity. Residual stresses are caused during welding due to steep thermal gradients, the solidification process, and the very distinct changes in material properties near the bimetallic interface. Weld residual stresses (WRS) can reach high levels within cladding and base material.

Post weld heat treatment (PWHT) is usually applied to reduce WRS. While being an effective mean to relax WRS within carbon and low-alloy steel [3], austenitic stainless steel is more heat resistant and is not expected to relax to the same extent [4] during a PWHT designed for carbon or low-alloy steel. WRS may therefore be substantially relaxed within the base material while a moderate effect can be expected within the cladding. Further, the residual stress state will also be influenced by any machining, subsequent pressure tests, and in some cases by operational and upset loads, which need to be evaluated in detail for each specific case.

Neutron embrittlement of the reactor pressure vessel steel generally limits the possible long-term operation of a nuclear power plant to e.g. 60 or 80 years. Sufficient remaining safety margins with respect to fracture has to be verified by structural integrity analyses that consider the plant surveillance tests results, defects in and near the cladding, the dimensioning load cases, and also residual stresses in the reactor pressure vessel. For these reasons good understanding and well documented estimates of the residual stresses in the cladding are very valuable.

Weld residual stresses can account for a large part of the total stress state when assessing the safety margin against fracture for RPVs and components, in particular for cases with low temperature and where the fracture toughness has been reduced as a consequence of irradiation embrittlement. When assessing the scenario of a pressurized thermal shock, or developing pressure-temperature limits, it is required to assume an internal surface crack. It is therefore important to investigate, substantiate and document the residual stresses, to use when

assessing the current status of a component, analysing fitness for continued operation, or considering long term operation. It is also noted that residual stresses in general influence crack growth mechanisms such as fatigue and stress corrosion cracking.

Depending on the welding process and base material, flaws have occurred in the low-alloy ferritic steel immediately beneath the cladding for some RPVs. Underclad cracks are located within the heat affected zone in the low-alloy steel beneath the cladding. These underclad cracks are for SA 508 Class 2 usually explained to be caused by reheating [5]. Another cause is cold cracking which has occurred in SA 508 Class 3 [6]. Understanding of the driving forces for the occurrence of these cracks is valuable. Further, when assessing the safety margin for these types of flaws, it is also essential to have detailed knowledge regarding the residual stress within the cladding and base material. This is particularly relevant with increased ageing and long term operation of existing facilities.

Thorough understanding of the processes leading to residual strains and stresses in clad reactor pressure vessels is challenging and is not limited to the levels of magnitude at a few individual positions but extends to full field information including distribution and gradients.

Examples of previously performed residual stress and strain measurements using different techniques are; the slitting, layer removal and the ring-core methods on clad mock-ups down to a limited depth [7], the layer removal method on plates and RPV cut-out specimen [8], by separation of the clad layer from the underlying material on blocks from an RPV shell segment [9], the ring-core method on RPV head cut-out specimen [10] and a cruciform clad specimen [11], the sectioning and deep-hole drilling methods through the full thickness of mock-ups [12], and the deep-hole drilling and neutron diffraction methods through the full thickness of a mock-up [13]. Residual stress and strain measurements are continuously reviewed and enhanced as measurement techniques are developed and improved.

The effect from pressure test is generally not included for mock-ups because it would require a pressure bearing vessel mock-up. An alternative would be decommissioned components although on-site measurements require adequate safety measures and cut out components undergo strain relief influencing the residual stress fields. The effect from pressure test and cut-outs may be analysed and accounted for by using numerical methods.

Numerical modelling can be used to predict residual stresses in specific components, for specific welding conditions, including effects of pressure tests and operational loads. Numerical predictions provide detailed full field results and can therefore offer a comprehensive basis for assessments and decisions concerning continued safe operation. However, it is of high importance that precise experimental measurement results are accessible for careful validation of numerical predictive methods. In addition to the residual stress and strain measurements, the validation case also needs to provide information about

welding process details, temperature response measurements and weld macrographs.

This report describes an experimental program where weld residual stresses and strains were measured on a simply supported strip cladded block manufactured as close to the actual welding procedures from the 1970s as possible. Multiple techniques were used to produce high resolution residual stress results through the thickness in an as-welded and post weld heat treated condition. The results also include detailed thermal responses at multiple locations close to the weld toe as well as weld macrographs. The measurements in this report provide valuable information of weld residual stresses for single layer weld deposited strip cladding and a basis for validation of numerical predictive methods.

2. Mock-up design

2.1 Base metal and weld overlay cladding

The mock-up was a low-alloy ferritic steel plate cladded with an austenitic stainless steel. It was intended to serve as a representation of a reactor pressure vessel, steam generator or pressurizer. Longitudinal cladding strips were sequentially deposited in one single layer. An illustration of the mock-up is shown in Figure 1.

The base metal consisted of two low-alloy steel plates of type SA-508 Class 3. Each plate had a thickness, length and width of approximately 156 mm, 500 mm and 250 mm, respectively. The two plates were butt welded together which resulted in a total plate width of 500 mm, and a butt weld in the length of the block at mid-width, see Figure 2. Records show that the welded plates were subject to post weld heat treatment at 620°C for 3 hours and 35 minutes. The welded and heat treated low-alloy steel plates were then cladded with austenitic stainless steel.

The cladding was achieved by submerged arc strip cladding using a combination of OK Flux 10.05 and OK Band 309L which, when applied as one single layer, results in a chemistry equivalent to stainless steel of type E308L. The width and thickness of the welding electrode were 60 mm and 0.5 mm, respectively. Deposited beads were approximately 70 mm wide and built approximately 5 mm height, see Figure 3.

Material properties for the low-alloy steel block are elastic material parameters based on [14] and yield strength at room temperature according to material certificates, see Table 1. Material properties used for the austenitic stainless steel cladding are according to Table 1. An isotropic modulus of elasticity of 195 GPa was assumed [15] for the cladding. It has been shown in e.g. [16] that the moduli in the as-welded condition can be dependent on orientation and deviate from a bulk value of 195 GPa by -15, -13, -25, and +12% in the longitudinal, transverse, normal and diagonal directions relative to the cladding strips, respectively. No mechanical testing were performed on the cladding material and the effect from anisotropy was not considered for the current measurements.

The final cladded mock-up is shown in Figure 4. Run-on and run-off plates, tack welded to the start and end sides of the block, were used to ensure steady state deposition along the welding direction. Plates were also tack welded to the sides of the block to prevent the first and last cladding strip to spill over the edges.

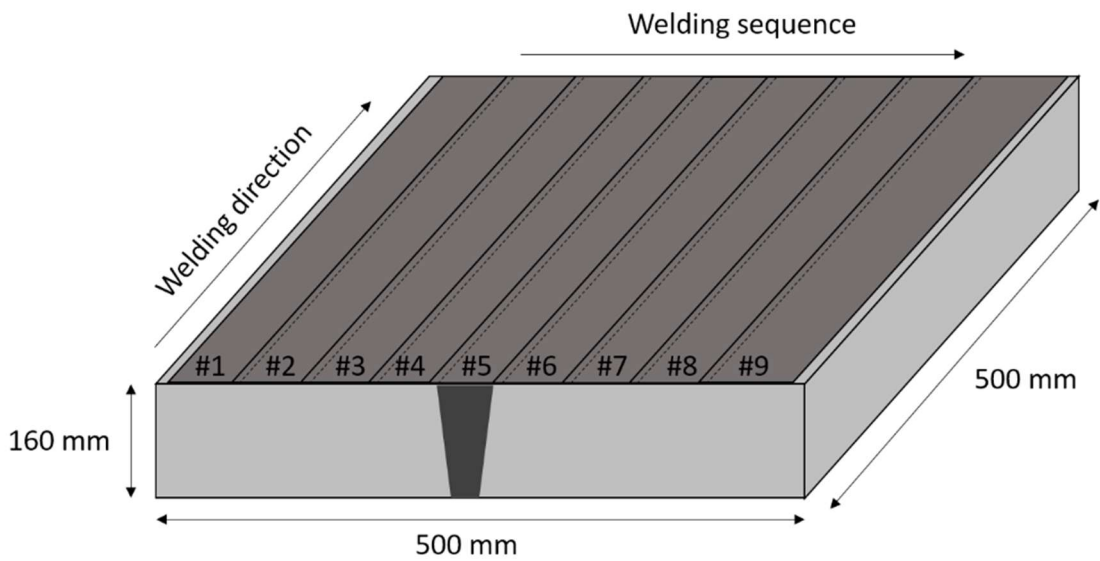


Figure 1 An illustration of welding direction, welding sequence and approximate dimensions.

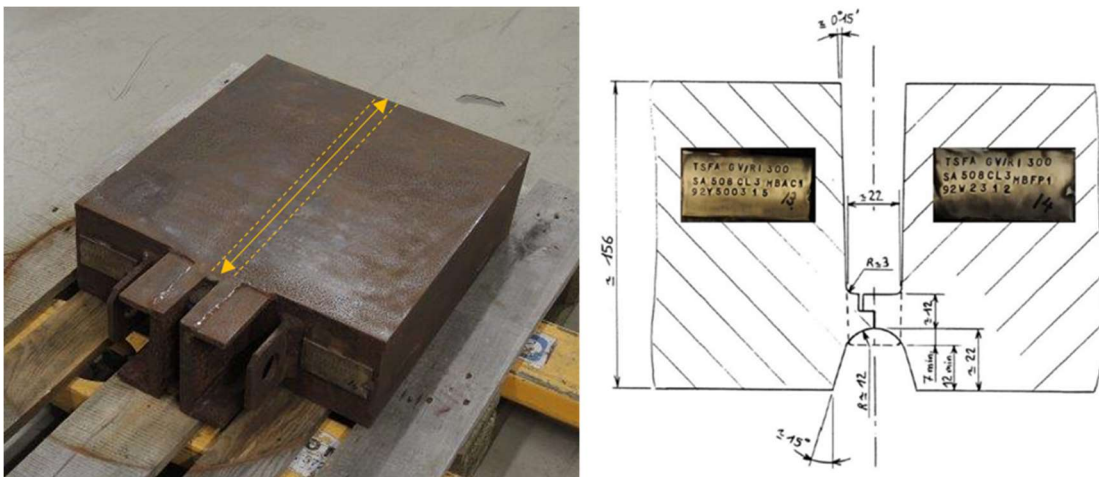


Figure 2 The base material consists of two low-alloy ferritic steel plates joined by a butt weld.

Table 1 Material properties for the base and cladding materials.

	Material	E [GPa]	ν [-]	σ_y [MPa]
Base	SA-508 Grade 3 Class 1 (formerly Class 3)	210	0.3	488
Cladding	E308L (Flux 10.05 + 309L)	195	0.3	402 (best estimate, as-welded)



Figure 3 The submerged arc strip cladding process resulted in deposited beads of approximately 70 mm width and 5 mm build height.

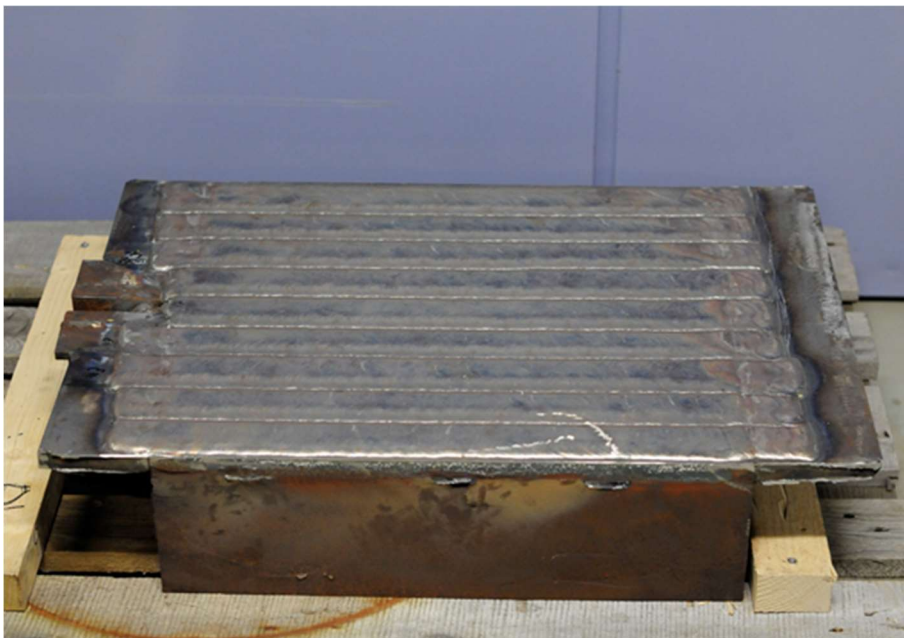


Figure 4 The cladded mock-up with nine strips, including attached run-on and run-off plates.

2.2 Submerged arc strip cladding

The submerged arc strip cladding has been used extensively since the 1960's. One or multiple arcs are created between the electrode and the base material. Molten slag is generated from the flux which protects the weld pool from oxidation and helps to produce a smooth cladding surface [17], see Figure 5. The arc between the electrode and the base material results in a relatively deep penetration with a dilution into the base material expected at approximately 18-25 percent [18]. As an example, a cladding layer which builds up a height of 5 mm would correspondingly indicate a penetration depth ranging between 1.1 mm and 1.7 mm.

Figure 6 shows a cross section extracted from the mock-up. The overview in Figure 6a shows the cladding, base material and a part of the pre-existing butt weld in the low-alloy steel. A close up view with etching for low-alloy steel is shown in Figure 6b. The heat affected zone can be perceived and two measurement readings show cladding layer thickness of 7.0 mm and 7.75 mm. A close up view with etching for stainless steel is shown in Figure 6c and the grain structure and strip overlap are visible.



Figure 5 Submerged arc welding of cladding strip #3 on the mock-up. Thermocouples are also seen in the pictures.

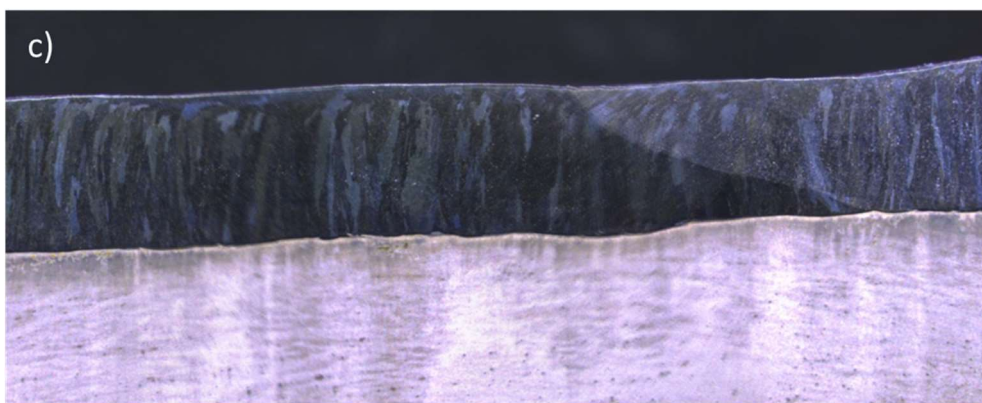
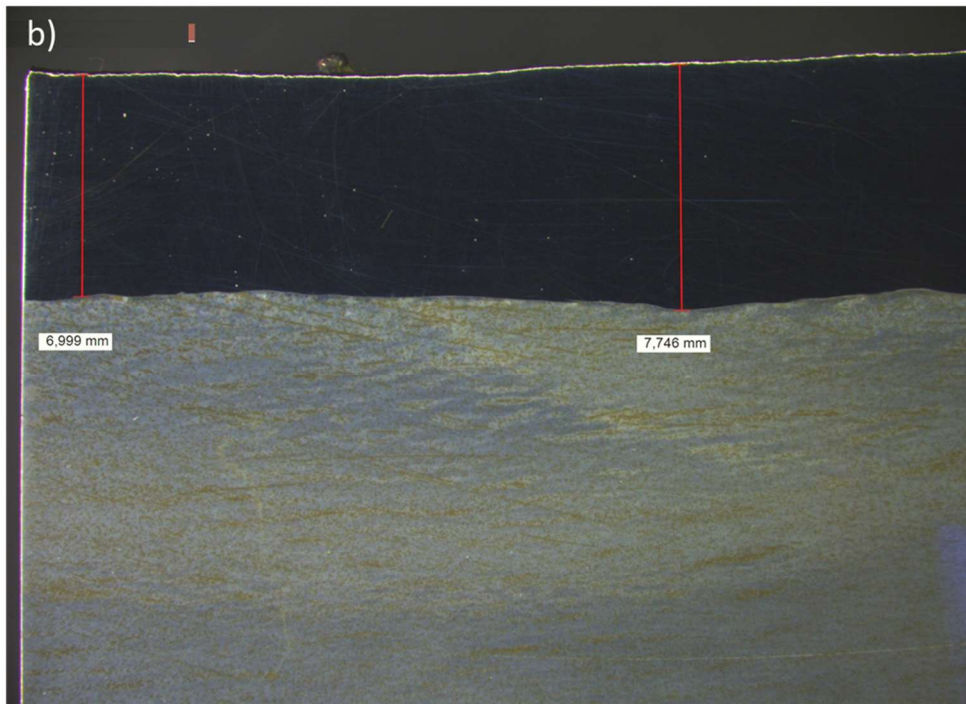


Figure 6 Cross section of a single layer strip cladding from the mock-up. a) Overview with the cladding, base material and part of its butt weld visible. b) Close up view with etching for low-alloy steel, including thickness measurements. c) Close up view with etching for stainless steel with strip overlap visible.

3. Overlay welding

3.1 Welding parameters

The project intended to follow an existing welding procedure specification (WPS) to accomplish a mock-up highly relevant to the nuclear industry. A WPS numbered SA-38-44 [19] was selected based on the chosen submerged arc cladding process. However, some modifications were necessary since the cladding strip and flux specified in the SA-38-44 are different from what was currently available for mock-up manufacturing. Preparatory test welding revealed that it was difficult to achieve a weld of sufficiently high quality with the electrical characteristics of SA-38-44. The current, potential and travel speed required to generate a weld with sufficient quality and build-up thickness were iteratively determined prior to the mock-up manufacturing, see Table 2.

Table 2 Welding parameters used during overlay welding.

Current [A]	Potential [V]	Travel speed [mm/min]	Heat input [kJ/mm]
750	29	130	10.04

3.2 Preheat and interpass temperatures

Preheating of the mock-up was achieved by means of ceramic heating elements and insulating blankets. At the beginning of welding, the insulating blankets were removed whereas the heating elements were retained to ensure an interpass temperature between 80°C and 125°C.

3.3 Post weld heat treatment

A post weld heat treatment in air environment was performed [20] according to common standard within the nuclear industry. A hold temperature of 620°C \pm 15°C was ensured for 8 hours. At temperatures above 300°C, the heating rate was \leq 45°C/h and the cooling rate was \leq 45°C/h. The process was controlled by use of four thermocouples attached to the component. Temperature readings digitized from paper and ink records are shown in Figure 7.

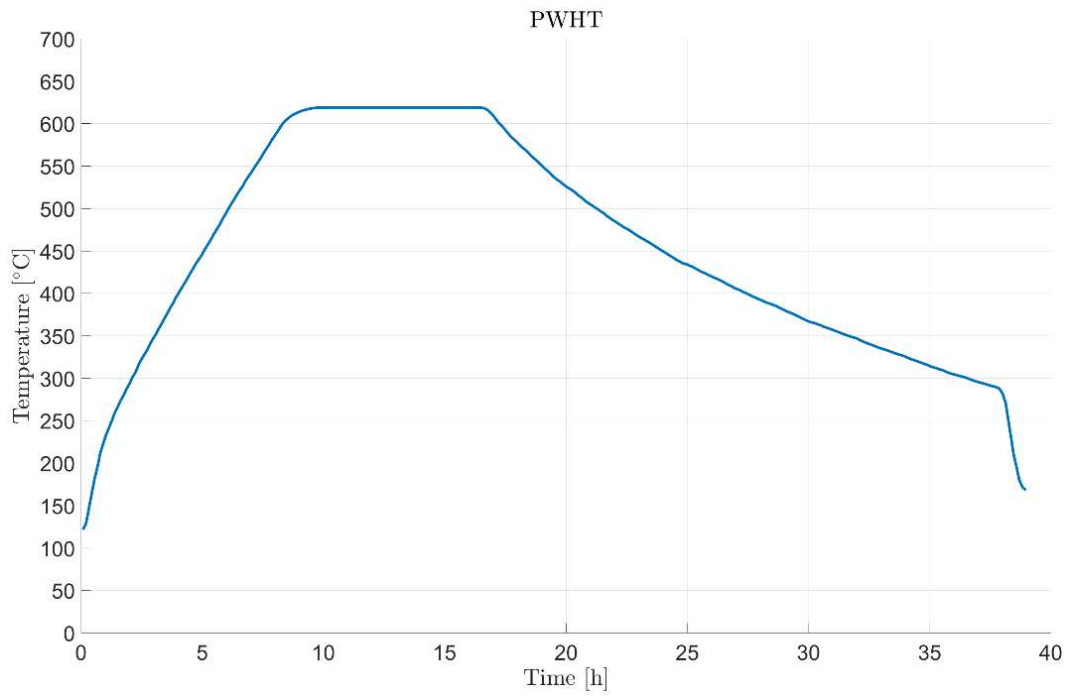


Figure 7 Record of temperature and time from the PWHT.

4. Temperature measurements

Thermocouples of type S with a specified temperature range 0°C to 1450°C were spot welded to the surface of the base material to measure the thermal response during welding. Precise measurements of the thermal response were carried out to record the temperature field close to each weld pass. The measurements serve as a reliable source to estimate the extension of the heat affected zone as well as for verification of numerical thermal simulations. The temperature field is expected to involve steep gradients in time as well as in physical space close to the weld where the highest temperatures within the base material occur.

The measurement system consisted of one Dewetron DEWE-2010 and one Dewetron DEWE-2600 which together provided 30 channels for simultaneous measurements. Analogous low pass filtering at 300 Hz, sampling at 1 kHz and decimation by a factor of 10 resulted in measurements at 100 Hz and enough margin with regard to aliasing and electrical disturbances. This instrumentation setup was regarded more than sufficient to capture the temperature gradients in the spatial and time domains.

Surface temperatures of the base material were expected to drop rapidly when the weld electrode has passed and fall below 750°C within 3 mm transverse to the fusion line. It was clear that the thermocouples had to be mounted as close to the fusion line as possible if the higher temperatures were to be successfully measured.

The thermocouple locations were planned according to the layout shown in Figure 8 and Figure 9. In total 30 thermocouples were mounted in area A and B along the 3rd pass. A predicted enveloped temperature profile in the transverse direction from the fusion line was used as guidance and a sequence of distances, important to the characterization of the maximum temperature, was established. The layout also had to consider that the thermocouples were to be manually mounted, with an accuracy estimated at approximately ± 0.5 mm, which required sufficient separation in the longitudinal direction. It was also essential to achieve redundancy in the measurement in terms of time and space since results should be consistent as function of distance from the weld toe as well as independent of position along the weld direction.

Thermocouples were mounted according to the layout which was, in turn, positioned relative a target line where the fusion line was expected, see Figure 10. It turned out to be a very challenging undertaking to hit the target line with high accuracy during welding due to the large irregularities along the welding direction, see Figure 11.

A thorough examination of photo documentation made it possible to manually measure the distance between the weld toe and each thermocouple. The thermal

responses in area A and B along the 3rd pass were gathered in one family of curves shown in Figure 12. The results exhibit some variation but capture the overall trend with sufficient accuracy. The thermal responses in area A and B along the 7th pass were also gathered in one family of curves shown in Figure 13. For this weld pass results were captured slightly closer to the weld toe. Some results from the 7th pass were omitted due to thermocouples being burned up and shortcut. There were also cases where thermocouples were trapped in solidified slag and ripped off the surface of the base material.

A magnification of Figure 11 reveals that the distance between the fusion line and the heat affected zone is approximately 2-3 mm on the surface. The heat affected zone is assumed to comprise areas of the base material which have experienced temperatures exceeding approximately 750 °C. The measured distance of 2-3 mm agrees with the thermal response given by the curves in Figure 12 and Figure 13.

The measured thermal response involves some uncertainty regarding the distance to the weld toe. The weld toe is fairly irregular and the transverse position may align with an irregularity which makes it difficult to assess the corresponding distance to the weld toe. Also, the spot weld has an unknown diameter and it is difficult to know exactly which point that corresponds to the actual measurement point.

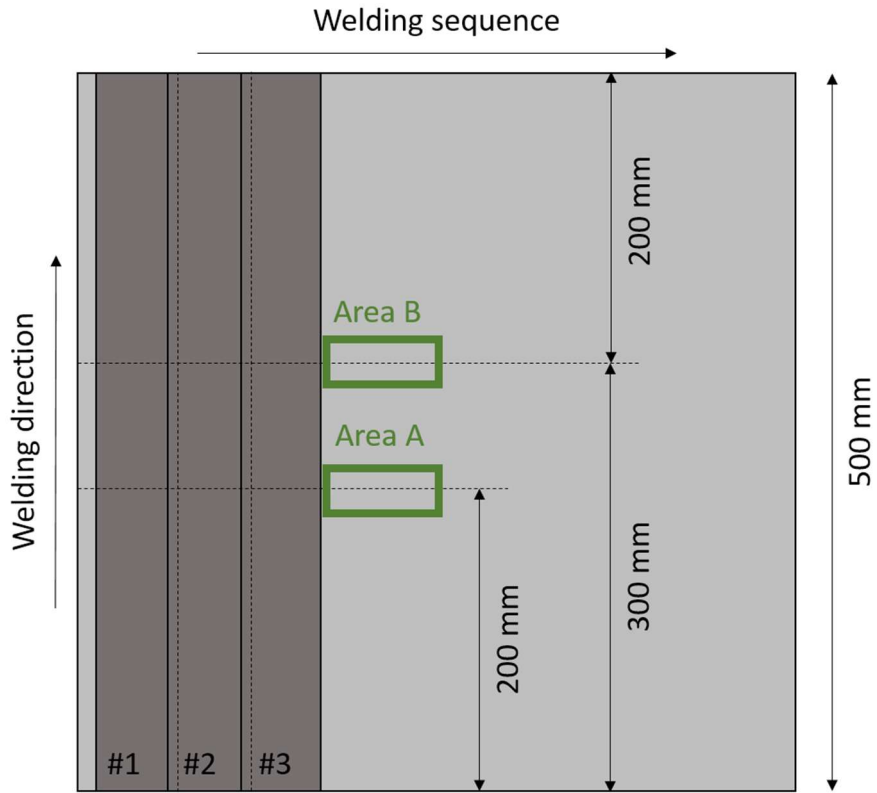


Figure 8 Thermocouples were mounted in Area A and B in order to achieve redundancy.

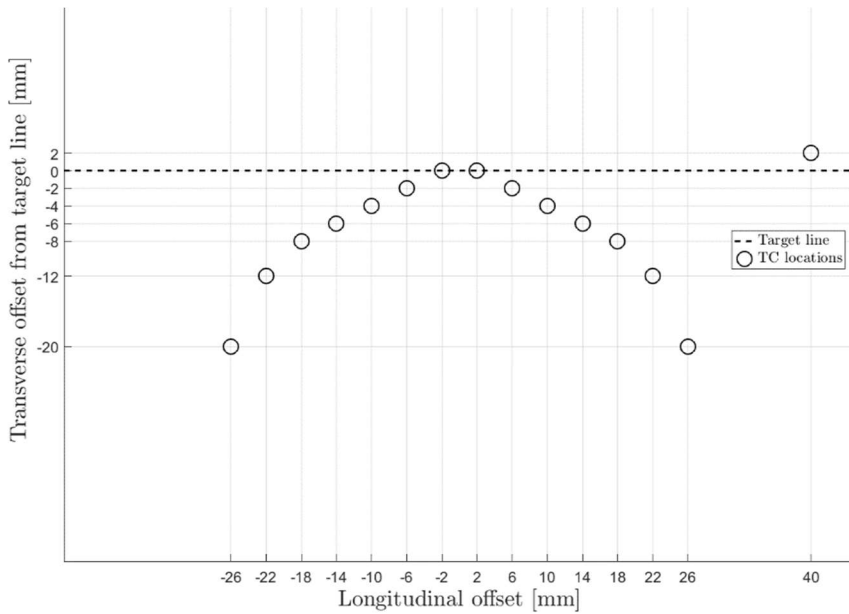


Figure 9 The thermocouples were mounted such that redundancy was achieved within each area.

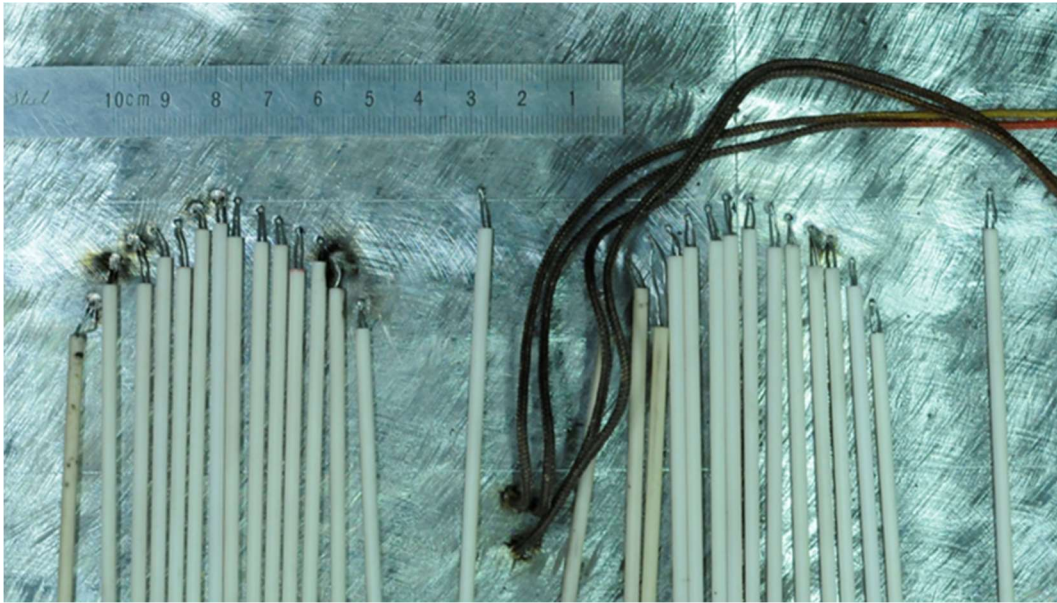


Figure 10 Thermocouples mounted according to the layout positioned relative the target line.

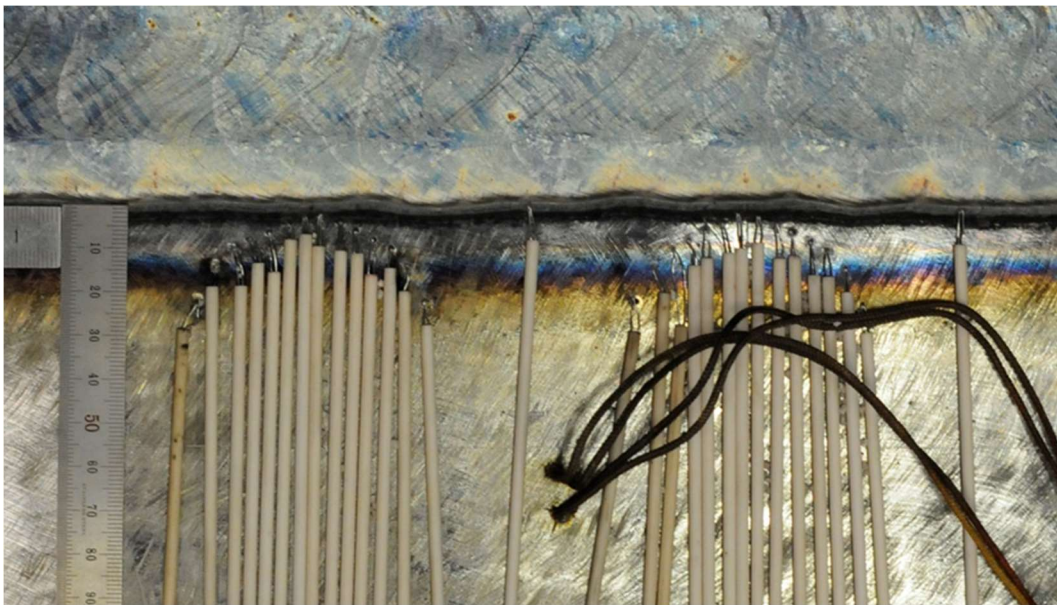


Figure 11 The resulting weld toe and its irregularities along the welding direction.

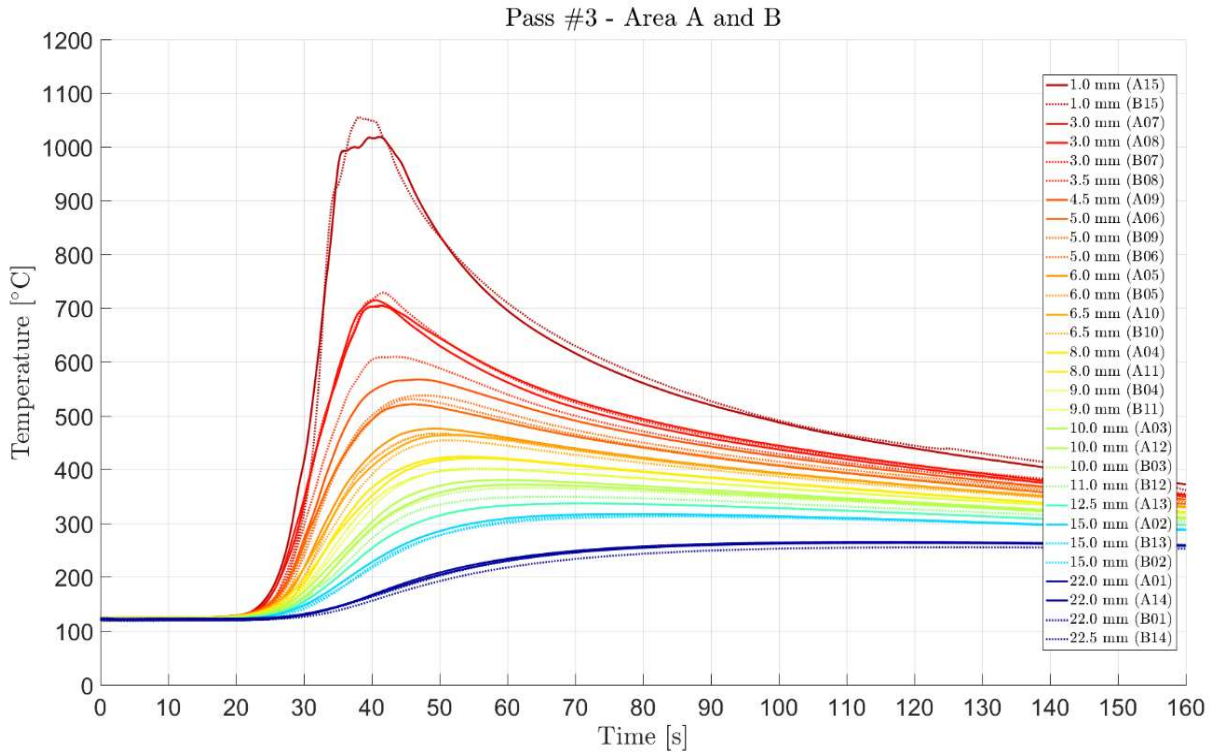


Figure 12 Thermal response transverse to the fusion line of the 3rd pass.

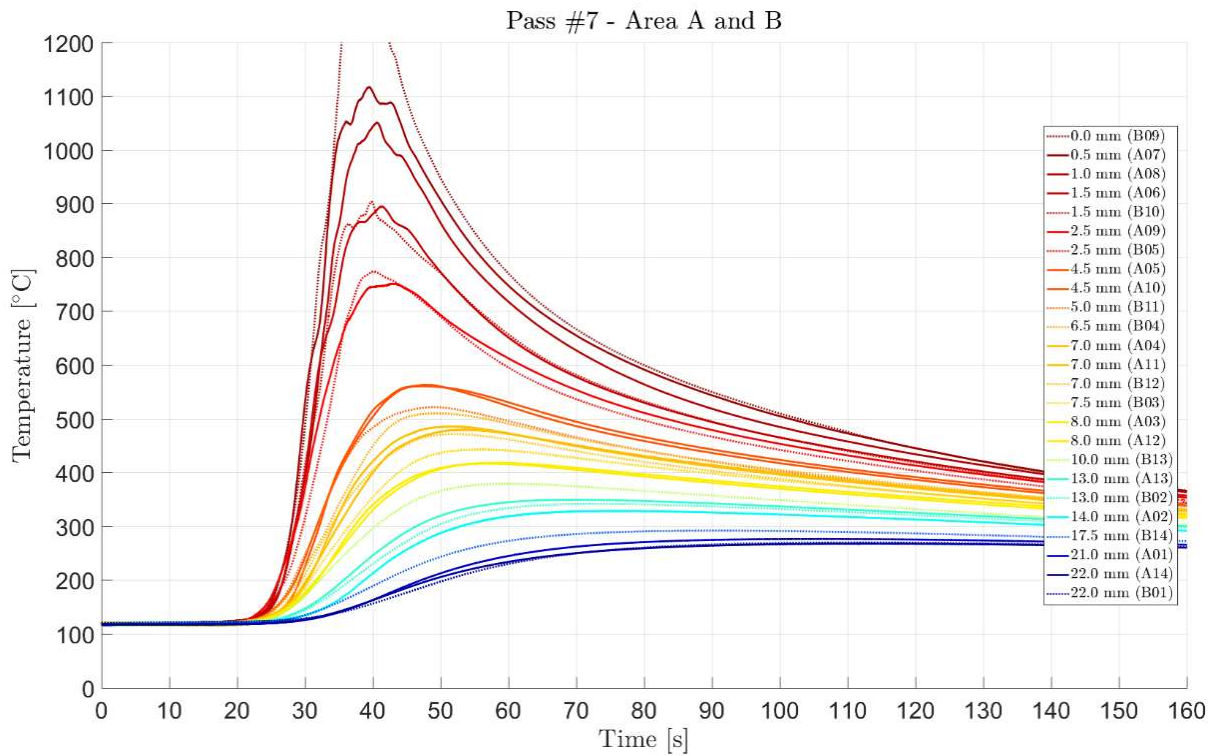


Figure 13 Thermal response transverse to the fusion line of the 7th pass.

5. Residual stress measurement techniques

5.1 Deep hole drilling

Deep hole drilling (DHD) is a technique for measurement of the bi-axial stresses through the thickness of a component based on strain release. An annular groove with a diameter of approximately 5 mm is trepanned around a central reference hole which acts as a strain gauge. The reference hole with a 1.5 mm diameter is drilled through the component and accurately measured before and after trepanning. Measurements before trepanning corresponds to a state where the residual stresses are present. The trepanning relieves the residual stresses which alters the shape of the reference hole. The difference is used to calculate the original residual stresses. The main steps of the procedure are detailed in e.g. [21] and one of the DHD measurements is illustrated in Figure 14.

If a component contains high magnitude residual stresses, the DHD technique may result in plastic deformation during trepanning. The deformation of the reference hole would in this case not serve as an accurate representation of the original residual stress field. When there are indications that plasticity will occur during measurement, an enhanced and incremental deep hole drilling (iDHD) will be used instead. Details of the iDHD technique are presented in [22].

The iDHD/DHD technique generates high accuracy residual stress measurement results through the thickness of the component. There are however sources of uncertainty. Surface effects that influence the reference hole may occur which influence the near surface results. Near surface effects that may alter the shape of the reference hole have been addressed in [23]. Further major sources of uncertainty have been published in [24] which involve i.e. calibration, curve-fit, misalignment and material uncertainty. Other sources of uncertainty such as triaxiality, additional plasticity effects, and independent length scales are difficult to characterize but have been considered negligible and have not been included in these experimental measurements. From previous calibration studies, the accuracy of iDHD/DHD was found to be as high as ± 30 MPa [25] assuming isotropic material properties, a Young's Modulus of 200 GPa and residual stresses that remain below 60% of the yield strength.

5.2 Incremental centre-hole drilling

Incremental centre-hole drilling (ICHHD) measures the bi-axial stresses near the surface based on strain release. Surface strains are measured concentrically around an incrementally machined shallow hole, see Figure 15. The residual stresses are determined by back calculation and a combination of experimental and numerical analyses according to an ASTM method [26] and [27].

The method is usually limited to a depth of 2 mm. Stress gradients and relief at depths may lead to inaccuracies since the strains are measured at the surface. The noise is most significant within the first and last 20% of the depth measured. An ICHD measurement is commonly carried out to depth 0.5 mm prior to each iDHD/DHD measurement.

5.3 Ring coring

Ring coring (RC) measures the bi-axial stresses near the surface based on mechanical strain release. An annular groove with a depth down to 5 mm is trepanned thus generating a central core, see Figure 16. A strain gauge rosette is used to monitor the intermittent surface strain relaxation at the core centre. Numerically determined influence coefficients are used to decompose the strain relaxation into residual stresses for each depth increment. The residual stresses measured are approximately an average of those acting across the cross-section of the central core.

Stress gradients and relief at depths may lead to inaccuracies since the strains are measured at the surface. The noise levels are significant within the first and last 20% of the depth measured due to low magnitudes of strain relaxation essentially increasing the noise to signal ratio. Details about the method can be found in [28] and [29].



Figure 14 Gun drilling at location 3A during the iDHD measurements [30].

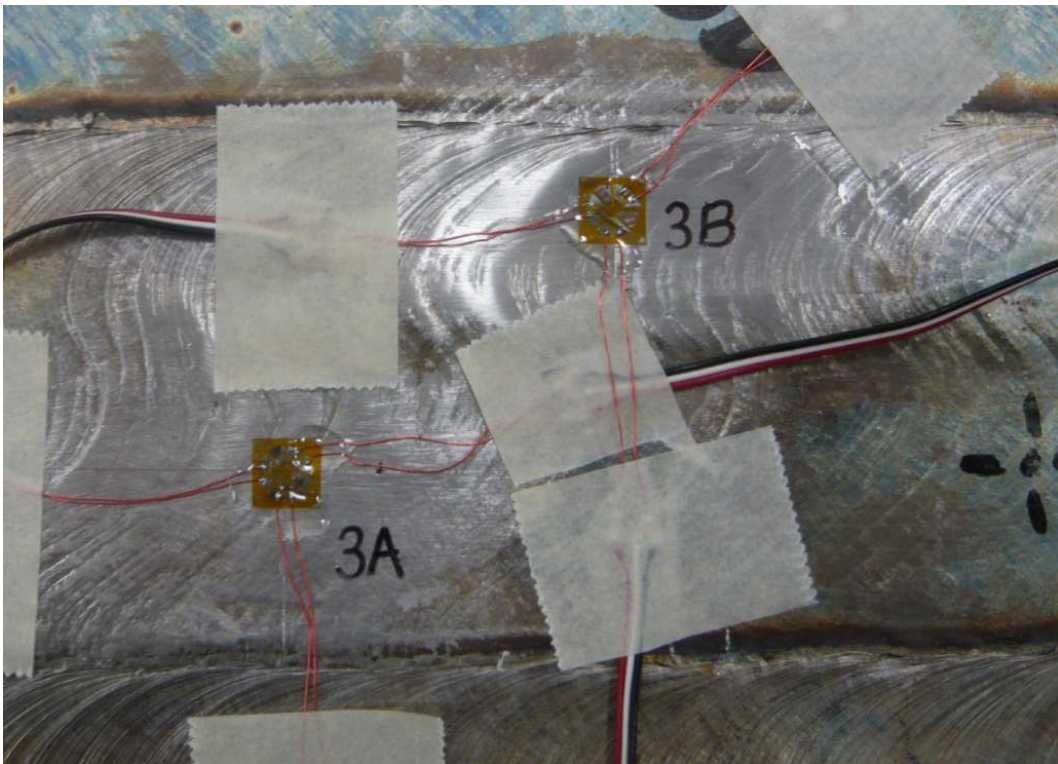


Figure 15 Strain gauge rosettes for the ICHD measurements [30].



Figure 16 Strain gauge rosette and central core after RC measurement [30].

6. Residual stress measurement locations

The mock-up plate is of finite width and length and contains a butt weld. The residual stress state of primary interest must be representative of a region without effects from edges or the butt weld. Thus, it is important to ensure that measurements are carried out in relevant positions with small influence from mock-up edges and the butt weld. The distance over which edge interaction vanishes has been estimated to be 100 mm. It has been assumed that the same condition is valid also regarding interaction from the butt weld, although this has not been investigated in detail. It was judged that the least interactions are to be expected mid-length in the cladding strips #3 and #7 which are separated from the mock-up edges and butt weld by distances of approximately 100 mm.

Residual stress measurements have been performed before and after post weld heat treatment (PWHT). The measurements before PWHT are expected to reveal the as-welded residual state whereas the measurements after PWHT are expected to show the amount of stress relief. The stainless-steel overlay is more temperature resistant compared to the low-alloy base material where the relaxation is mainly expected to take place.

The cladding was deposited in strips resulting in almost constant thickness but with slightly varying widths and overlaps. Each overlap implies a region that has

experienced an additional thermal cycle which may have altered the residual state resulting from the first weld pass. This alteration could imply a deviation in residual stress levels as well as a change of the residual stress profile. Measurements were carried out at the mid of the strip as well as at the mid of the overlap location to detect potential deviations.

A first set of measurements were performed in cladding strip #3 with the block in its as-welded state, for a position mid-strip and a position mid-overlap. The block was then sent out for a PWHT. A second set of measurements in cladding strip #7 commenced after PWHT. One last measurement was carried out in cladding strip #5 and at mid-length of the plate butt weld.

The measurement locations in cladding strips #3 and #7 are shown in Figure 17. Measurements by iDHD/DHD (including ICHD) have been carried out mid-strip (A) and mid-overlap (B). RC measurements have been carried out mid-strip (C).

The measurement location in cladding strip #5 is shown in Figure 18. This measurement was carried out at the mid-strip location, and in line with the mid-strip locations in the cladding strips #3 and #7. But most importantly, it was carried out at the weld centre line of the plate butt weld, which was the main motivation for this measurement. The butt weld location was known approximately but due to the 22 mm butt weld gap and that the measurement was to be performed as close as possible to the weld centre line, an etchant 2% Nital solution was used on the clad side and bottom surfaces in order to get precise information on its actual location, see Figure 18.

In total, two RC measurements and five iDHD/DHD (including ICHD) were performed. The RC and iDHD/DHD measurements obtained the longitudinal and transverse residual stresses with respect to the cladding direction and the associated in-plane shear residual stresses. For each phase of measurements, the ICHD measurements were carried out prior to the iDHD/DHD measurements and the RC measurements were carried out last. All locations where residual stress measurements have been performed are shown in Figure 19.

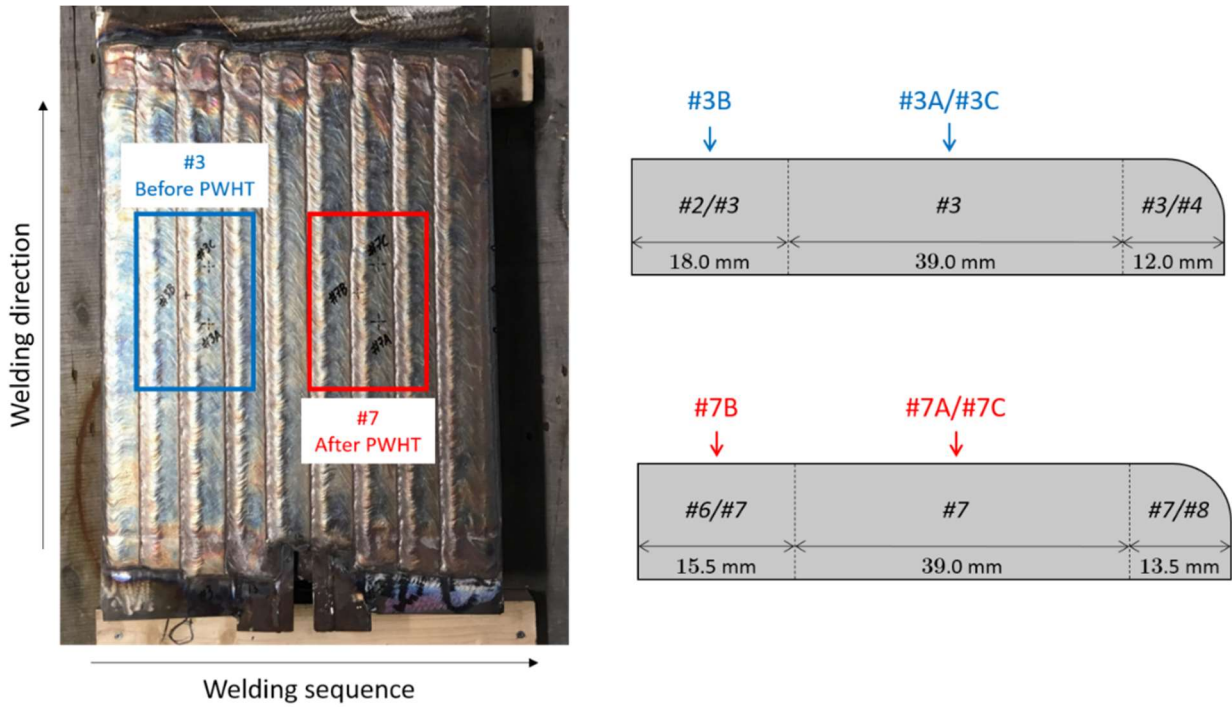


Figure 17 Measurement locations in strip #3 before PWHT and in strip #7 after PWHT.

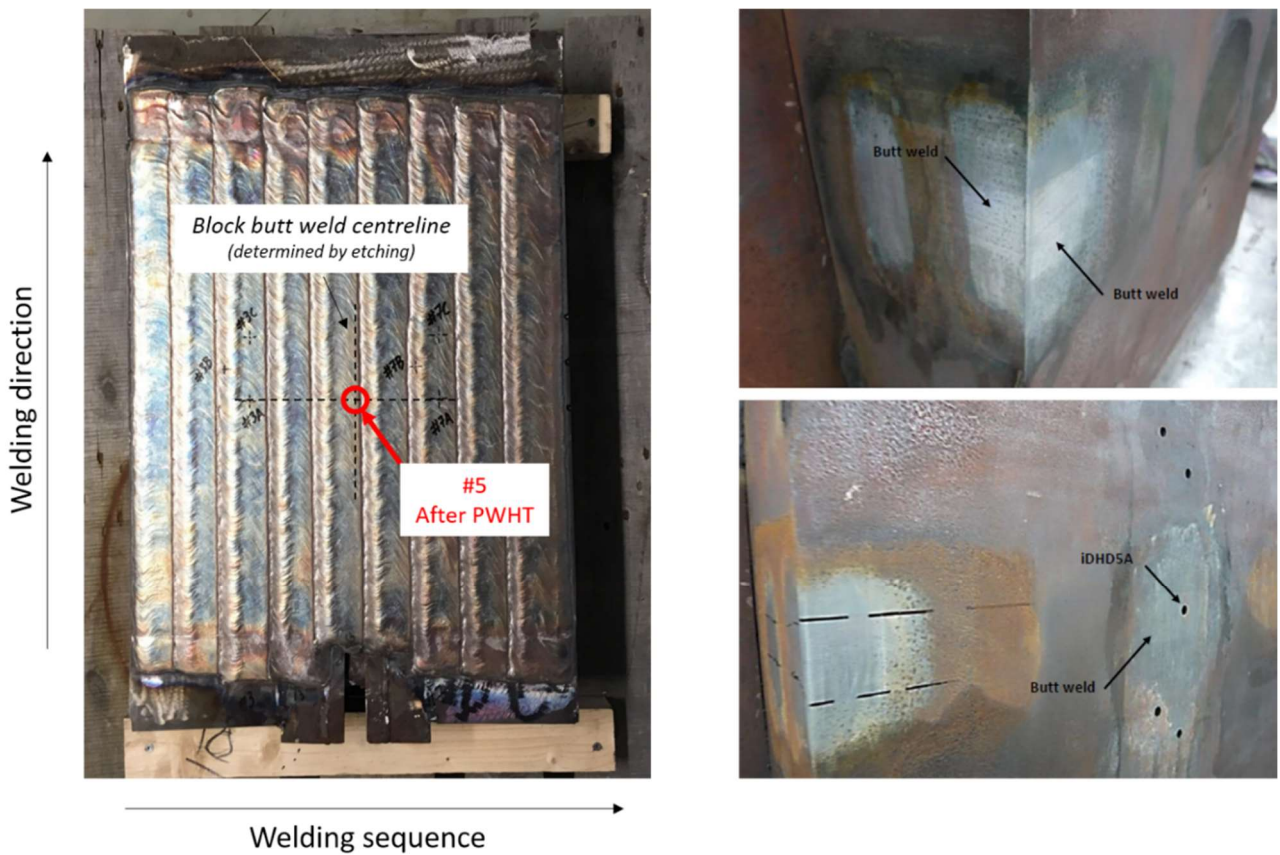


Figure 18 Measurements were carried out in strip #5 at the plate butt weld after PWHT.

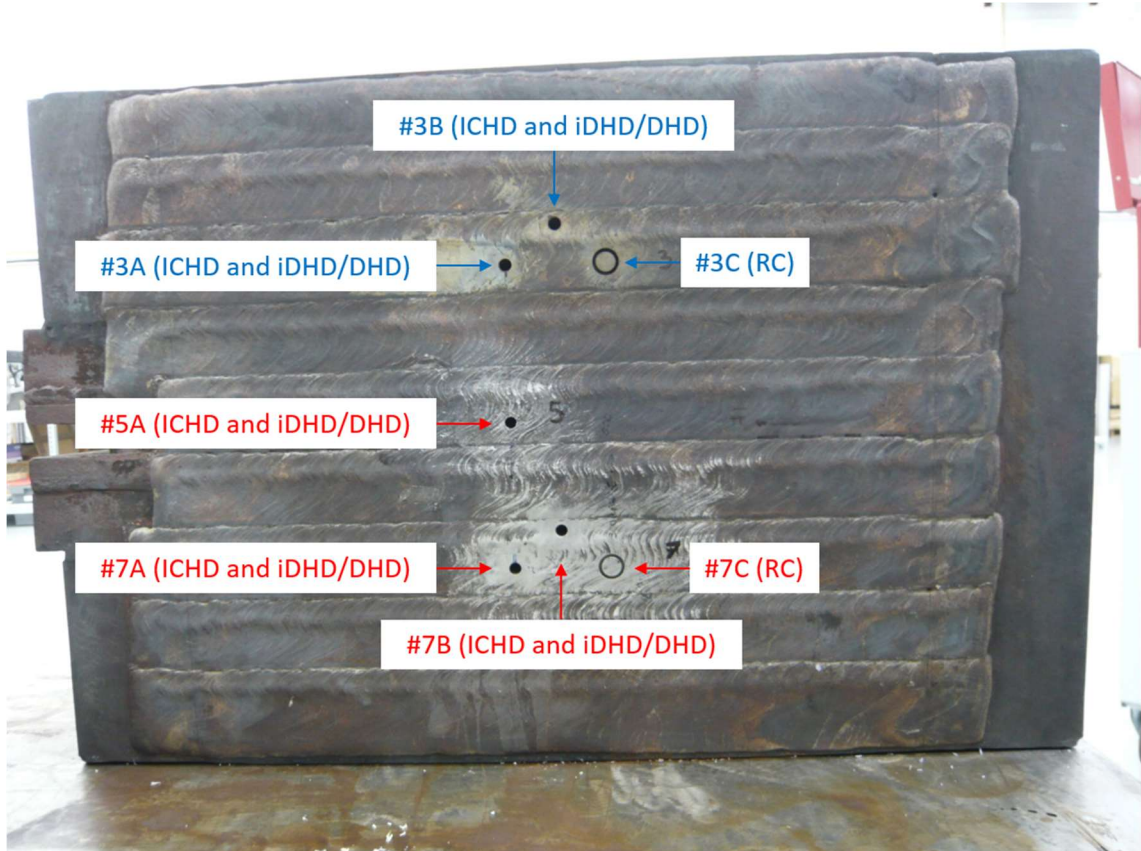


Figure 19 All locations where residual stress measurements were performed [30].

7. Residual stress measurement results

This section summarises the results for measurement of residual stresses through the thickness, based on the more detailed documentation in [30].

The residual stresses were determined using a Young's Modulus of 195 GPa and a Poisson's ratio of 0.3 for the cladding and a Young's Modulus of 210 GPa and a Poisson's ratio of 0.3 for the base metal, see Table 1.

Two RC measurements were carried out and smooth results were obtained but significant differences were observed compared to the results from iDHD/DHD. Plastic relaxation during the RC measurement was believed to be the root cause for this discrepancy. The RC measurement results were considered to be unreliable and were not presented in [30].

ICHD measurements were carried out down to a depth of 0.5 mm prior to each iDHD/DHD measurement. Results in the first and last 20% of the measurement depth have been omitted due to procedure uncertainties.

The iDHD/DHD results presented in [30] are a combination of both the iDHD and standard DHD techniques depending on the degree of plastic strain relaxation during the measurement process. Only iDHD results have been presented in regions with plastic relaxation where the DHD results were judged inaccurate. Otherwise, only the DHD results were presented as the DHD technique provides a higher spatial resolution.

7.1 Cladded block in as-welded state

7.1.1 Location #3A - mid-strip, as-welded

The longitudinal and transverse residual stresses through the thickness at the mid-strip location #3A are shown in Figure 20 for the as-welded state of cladding. The residual stresses were obtained from iDHD/DHD and are given as a function of distance from the nominal interface between the clad and base metal.

The iDHD/DHD measurements showed an equi-biaxial residual stress state throughout, with the transverse residual stresses being slightly larger than the longitudinal residual stresses within the cladding, and vice versa through the thickness of the base metal. The residual stresses started in tension from about 170 MPa and 120 MPa respectively in the transverse and longitudinal directions at a depth of 0.6 mm. The stresses increased to about 245 MPa and 200 MPa, respectively, at a depth of about 2.2 mm within the cladding. Both the transverse and longitudinal residual stresses then sharply decreased into a compressive state of around -20 MPa at a depth of 7 mm to 9 mm (approximately 2 mm to 4 mm underneath the clad to base metal interface). The residual stresses sharply increased again and reached maxima of around 415 MPa at a depth of 17.2 mm.

The residual stresses then decreased again and reached a minimum of -164 MPa and -187 MPa, respectively, at about 40 mm depth into the base metal. Finally, the residual stresses increased linearly to about 150 MPa and 200 MPa, respectively, near to the back surface of the block.

Figure 21 shows the longitudinal and transverse residual stresses from the combination of the ICHD and iDHD/DHD measurements on a base 10 logarithmic scale.

The ICHD measurement for very shallow depth show transverse and longitudinal residual stresses that started in compression at around -200 MPa. The stresses then increased linearly to a maximum value of around 100 MPa at a depth of 0.2 mm. Finally the measured residual stresses decreased to almost zero at a depth of 0.5 mm.

7.1.2 Location #3B - mid-overlap, as-welded

The longitudinal and transverse residual stresses through the thickness at the mid-overlap location #3B are shown in Figure 22 for the as-welded state of cladding. The residual stresses were obtained from iDHD/DHD and are given as a function of distance from the nominal interface between the clad and base metal.

The iDHD/DHD measurement showed an equi-biaxial residual stress state throughout, with the transverse residual stresses being slightly larger than the longitudinal residual stresses within the cladding, and vice versa through the thickness of the base metal. The residual stresses started in tension from about 280 MPa and 195 MPa respectively in the transverse and longitudinal directions at a depth of 1.0 mm. The stresses increased to about 350 MPa and 275 MPa, respectively, at a depth of about 2.2 mm within the cladding. Both the transverse and longitudinal residual stresses then sharply decreased into a compressive state of around -10 MPa at a depth of around 7 mm (approximately 2 mm underneath the clad to base metal interface). The residual stresses sharply increased again and reached maxima of around 410 and 420 MPa, respectively, at a depth of 12.6 mm. The residual stresses then decreased again and reached a minimum of about -205 MPa and -250 MPa, respectively. Finally, the residual stresses increased linearly to about 100 MPa and 160 MPa, respectively, near to the back surface of the block.

Figure 23 shows the longitudinal and transverse residual stresses from the combination of the ICHD and iDHD/DHD measurements on a base 10 logarithmic scale.

The ICHD measurements obtained transverse residual stresses that started in large compression for the very shallow depths. The measured stresses then increased linearly to a maximum value of about 340 MPa and 100 MPa respectively in the transverse and longitudinal directions at a depth of 0.125 mm. The residual

stresses gradually decreased and plateaued at about 150 MPa and 50 MPa, respectively.

7.2 Cladded block in post-weld heat treated state

7.2.1 Location #7A - mid-strip, after PWHT

The residual stresses through the thickness at the mid-strip location #7A are shown in Figure 24 after PWHT. The residual stresses were obtained from iDHD/DHD and are given as a function of distance from the nominal interface between the clad and base metal.

The iDHD/DHD measurement showed an equi-biaxial residual stress state throughout, with significant tension within the cladding and low magnitude residual stresses in the base metal. The residual stresses started in tension from about 215 MPa and 200 MPa respectively in the transverse and longitudinal directions at a depth of 1.0 mm. The stresses increased to around 240 MPa and 245 MPa, respectively, at a depth of about 2.2 mm within the cladding. Both the transverse and longitudinal residual stresses then sharply decreased and reduced to a slightly compressive state immediately beneath the interface. The residual stresses oscillated between -50 MPa and +50 MPa in the base material. Finally, the residual stresses increased slowly to about 65 MPa and 45 MPa, respectively, near to the back surface of the block. A compressive peak in the residual stresses of about -90 MPa was found at a depth of 33 mm.

Figure 25 shows the longitudinal and transverse residual stresses from the combination of the ICHD and iDHD/DHD measurements on a base 10 logarithmic scale.

The ICHD measurements obtained transverse and longitudinal residual stresses that started in compression at around -50 MPa and tension at around 50 MPa for the very shallow depths. The stresses then increased and plateaued at 0.2 mm at a maximum value of around 150 MPa at a depth between 0.15 mm and 0.3 mm. The residual stresses finally decreased to reach almost zero at a depth of 0.5 mm.

7.2.2 Location #7B - mid-overlap, after PWHT

The residual stresses through the thickness at the mid-overlap location #7B are shown in Figure 26 after PWHT. The residual stresses were obtained from iDHD/DHD and are given as a function of distance from the nominal interface between the clad and base metal

The iDHD/DHD measurement showed an equi-biaxial residual stress state throughout, with significant tension within the cladding and low magnitude residual stresses in the base metal. The residual stresses started in tension from about 225 MPa and 245 MPa respectively in the transverse and longitudinal directions at a depth of 0.8 mm. The stresses increased to about 250 MPa and 280 MPa,

respectively, at a depth of about 2.2 mm within the cladding. Both the transverse and longitudinal residual stresses then sharply decreased and reduced to a slightly compressive state immediately beneath the interface. The residual stresses oscillated between -50 MPa and +50 MPa in the base material. Finally, the residual stresses increased slowly to about 85 MPa and 110 MPa, respectively, near to the back surface of the block. A compressive peak in the residual stresses of about -140 MPa and -110 MPa, respectively, was found at a depth of 38 mm.

Figure 27 shows the longitudinal and transverse residual stresses from the combination of the ICHD and iDHD/DHD measurements on a base 10 logarithmic scale.

The residual stresses obtained from the ICHD measurement at depths from 0.025 mm to 0.15 mm were omitted due to strongly unreliable data and abnormally increased uncertainty. The stresses decreased from almost zero to about -70 MPa at a depth of 0.25 mm. The residual stresses finally increased to reach almost 100 MPa at a depth of 0.5 mm.

7.2.3 Location #5A - mid-strip, at butt weld, after PWHT

The residual stresses through the thickness at the mid-strip location #5A at the butt weld in the steel plates are shown in Figure 28 after PWHT. The residual stresses were obtained from iDHD/DHD and are given as a function of distance from the nominal interface between the clad and base metal

The iDHD/DHD measurement showed an equi-biaxial residual stress state throughout, with significant tension within the cladding and low magnitude residual stresses in the base metal. The residual stresses started in tension from about 225 MPa and 240 MPa respectively in the transverse and longitudinal directions at a depth of 0.8 mm. The stresses increased to about 285 MPa and 300 MPa, respectively, at a depth of about 2.4 mm within the cladding. Both the transverse and longitudinal residual stresses then sharply decreased and reduced to almost zero immediately beneath the interface. The residual stresses oscillated between -40 MPa and +60 MPa in the base material. Finally, the residual stresses increased to about 135 MPa and 175 MPa, respectively, near to the back surface of the block. Unlike the measurements in the locations #7A and #7B, no compressive peak in the residual stresses was observed.

Figure 29 shows the longitudinal and transverse residual stresses from the combination of the ICHD and iDHD/DHD measurements on a base 10 logarithmic scale.

The ICHD measurement obtained for the very shallow depths transverse, longitudinal and shear residual stresses that started in compression exceeding -250 MPa. The stresses then increased to a maximum value of around 190 MPa at a depth of 0.15 mm for the transverse stress and 160 MPa at a depth of 0.225 mm for the longitudinal stress. Finally the measured residual stresses reached almost zero at a depth of 0.5 mm.

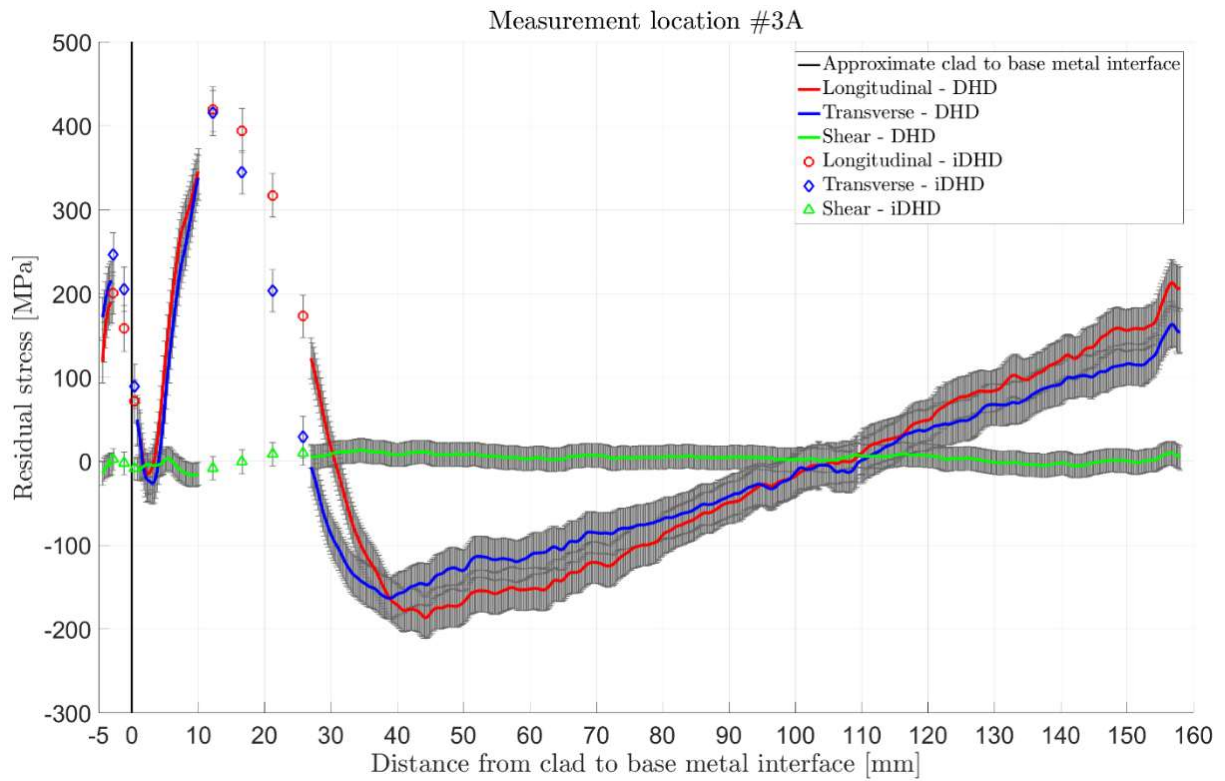


Figure 20 Residual stress measured by iDHD/DHD at location #3A (mid-strip) as-welded.

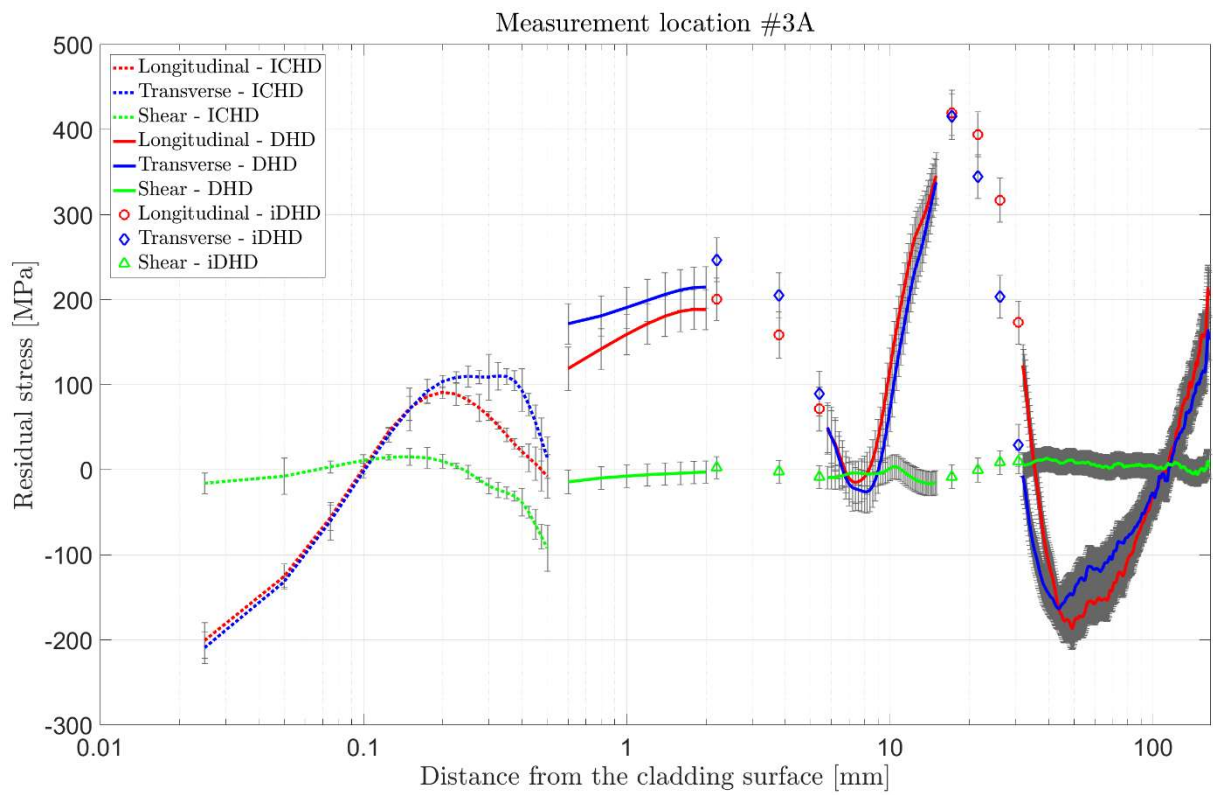


Figure 21 Residual stress measured by ICHD and iDHD/DHD at location #3A (mid-strip) as-welded.

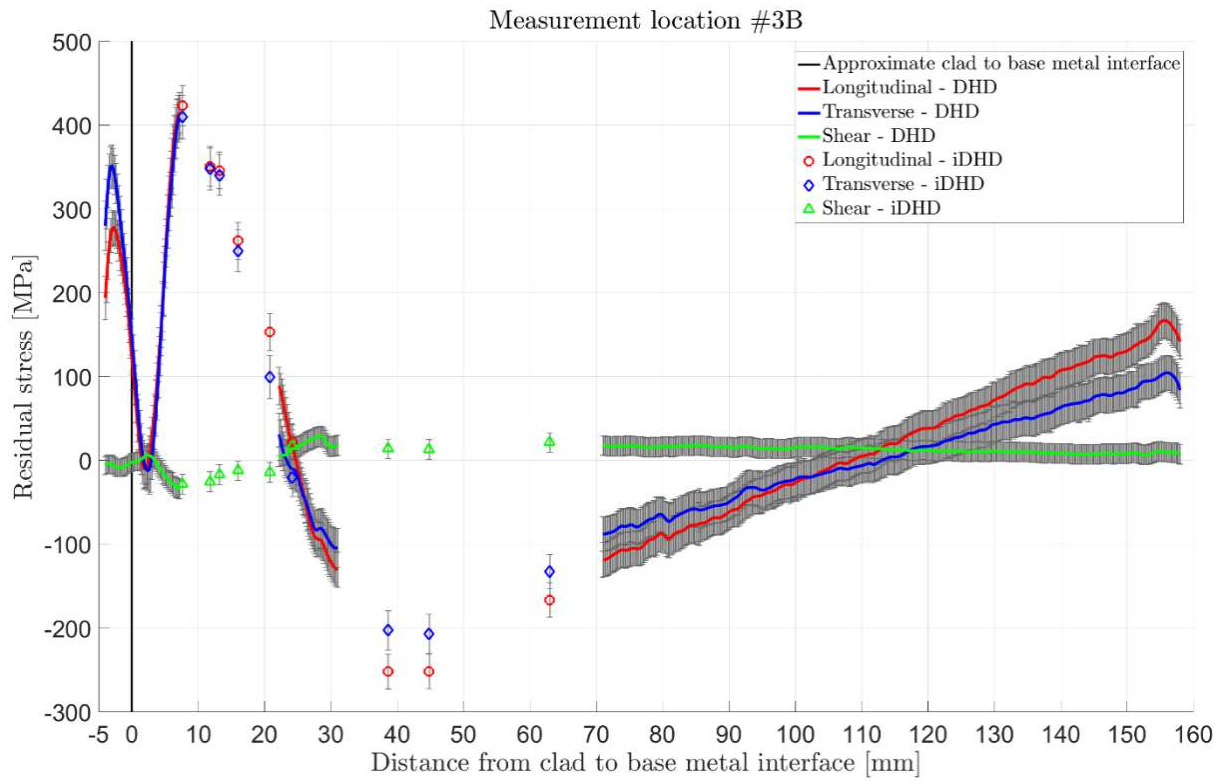


Figure 22 Residual stress measured by iDHD/DHD at location #3B (mid-overlap) as-welded.

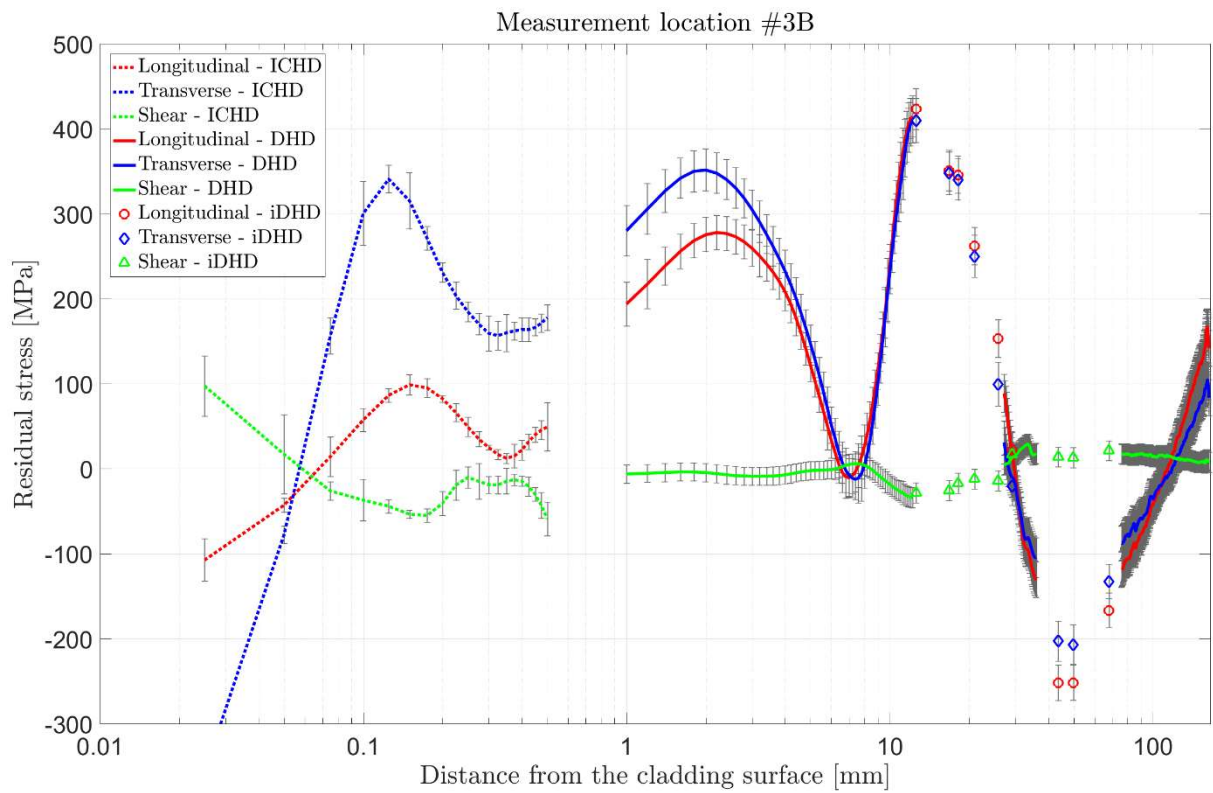


Figure 23 Residual stress measured by ICHD and iDHD/DHD at location #3B (mid-overlap) as-welded

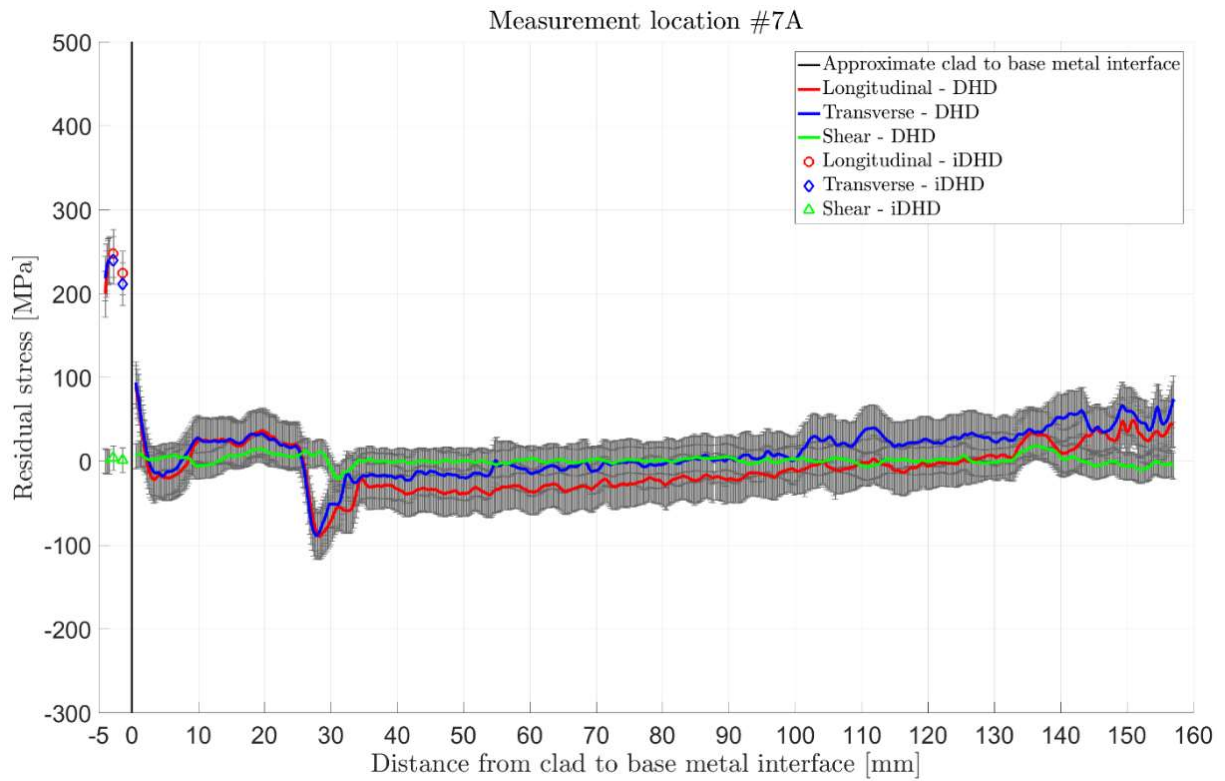


Figure 24 Residual stress measured by iDHD/DHD at location #7A (mid-strip) after PWHT.

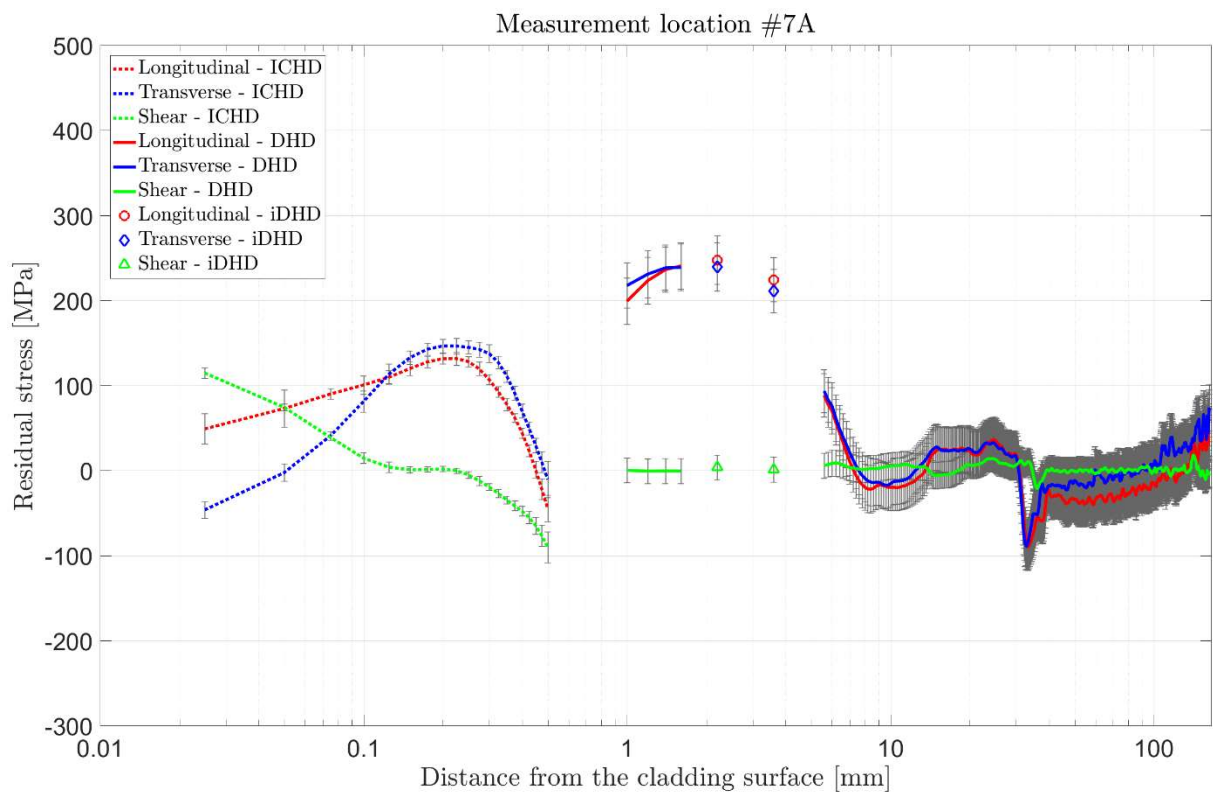


Figure 25 Residual stress measured by ICHD and iDHD/DHD at location #7A (mid-strip) after PWHT.

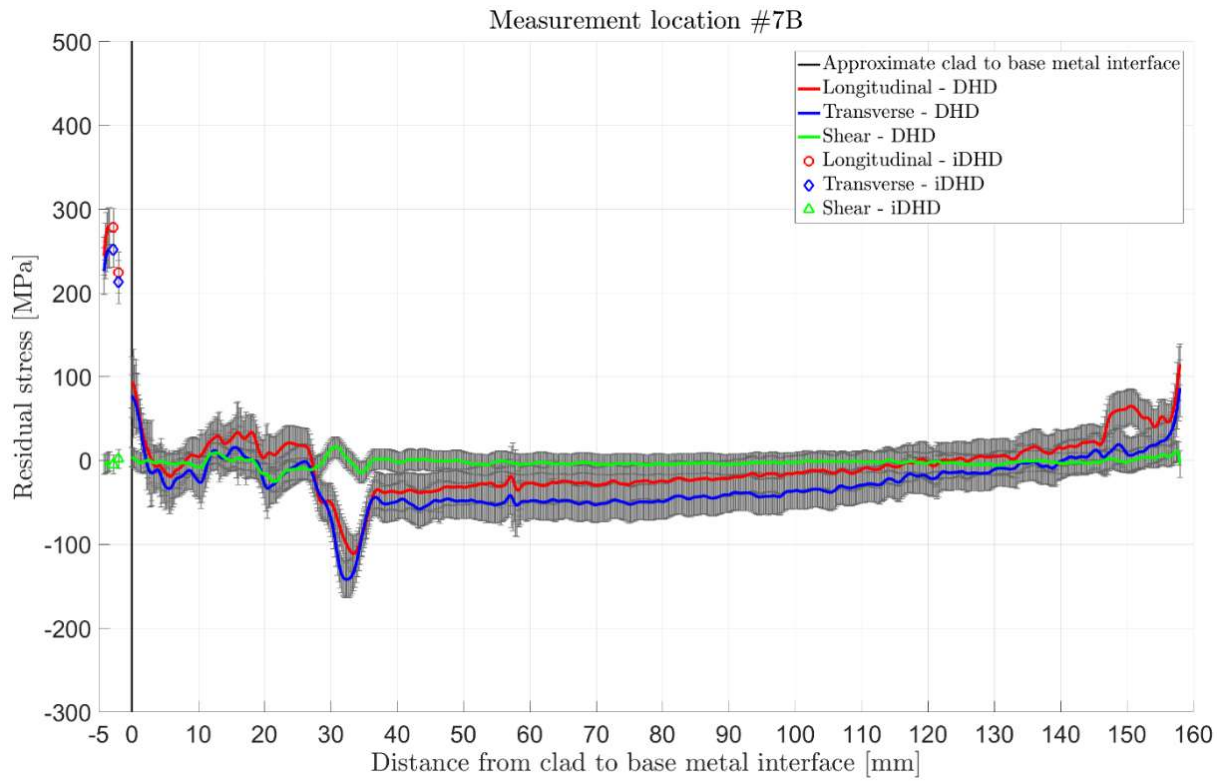


Figure 26 Residual stress measured by iDHD/DHD at location #7B (mid-overlap) after PWHT.

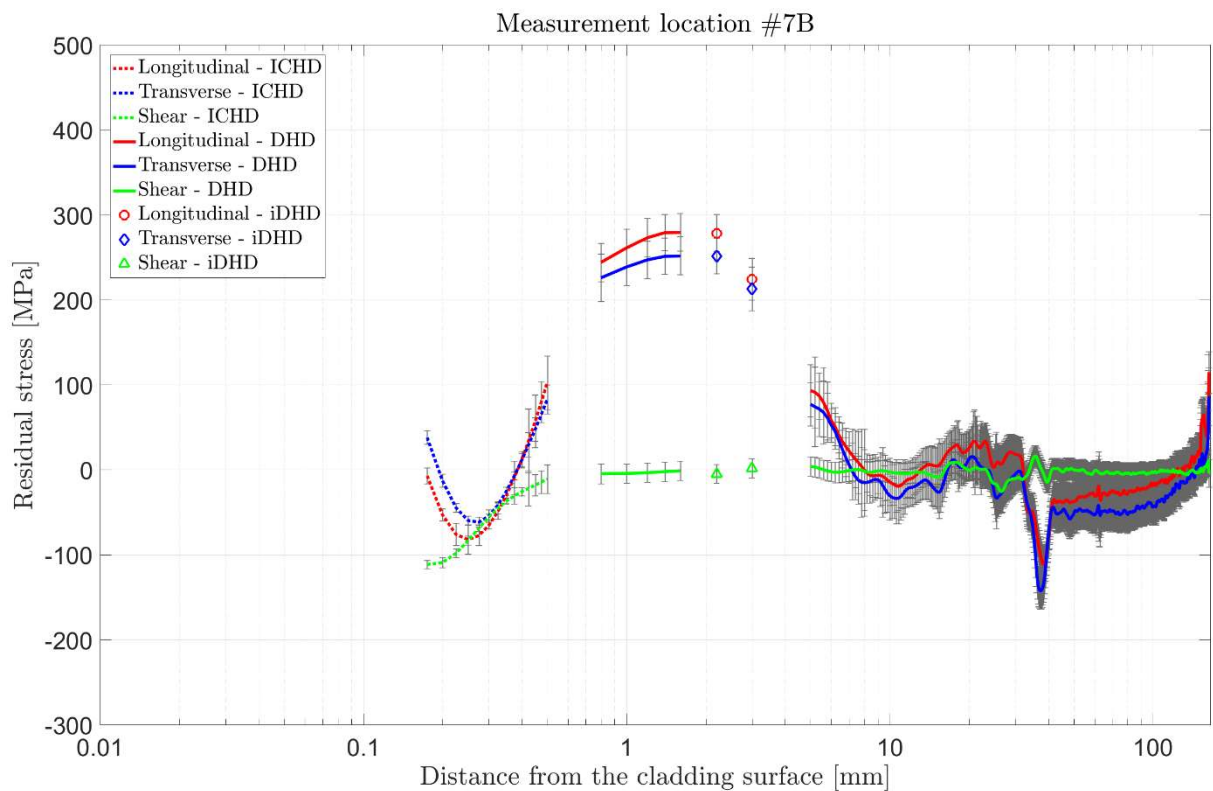


Figure 27 Residual stress measured by ICHD and iDHD/DHD at location #7B (mid-overlap) after PWHT.

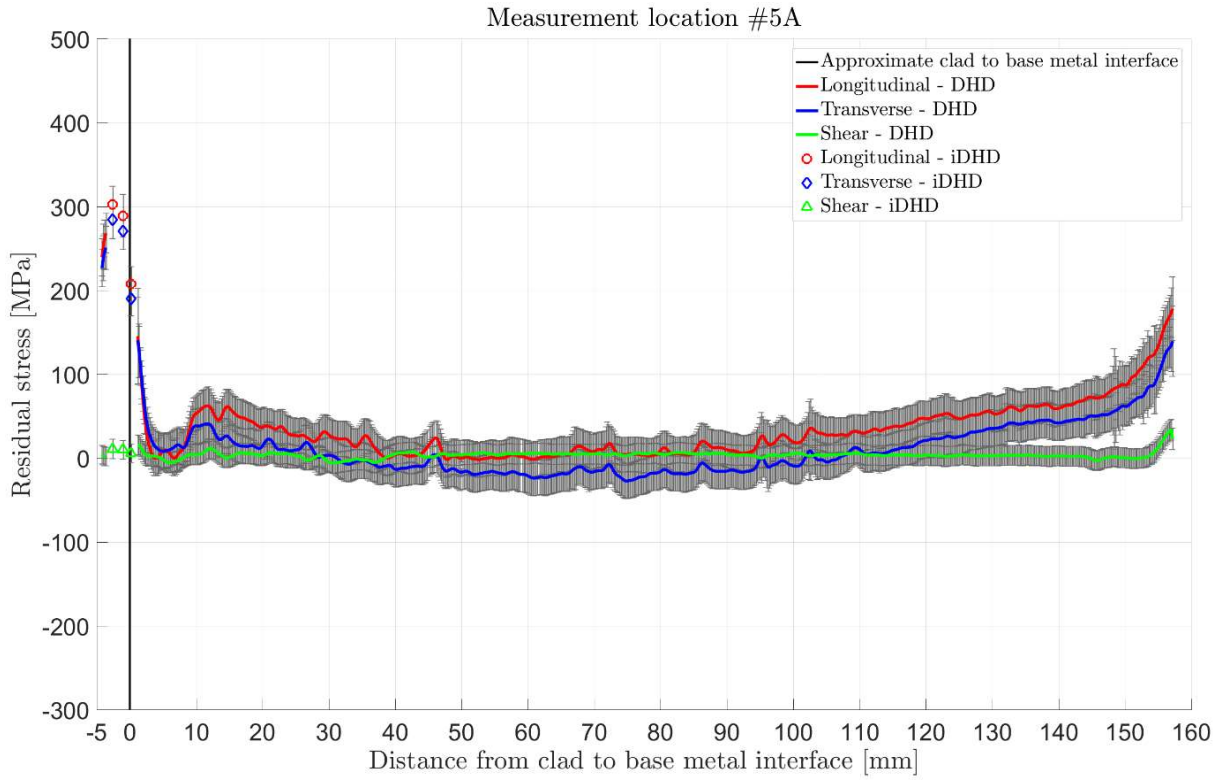


Figure 28 Residual stress measured by iDHD/DHD at location #5A (mid-strip, at butt weld) after PWHT.

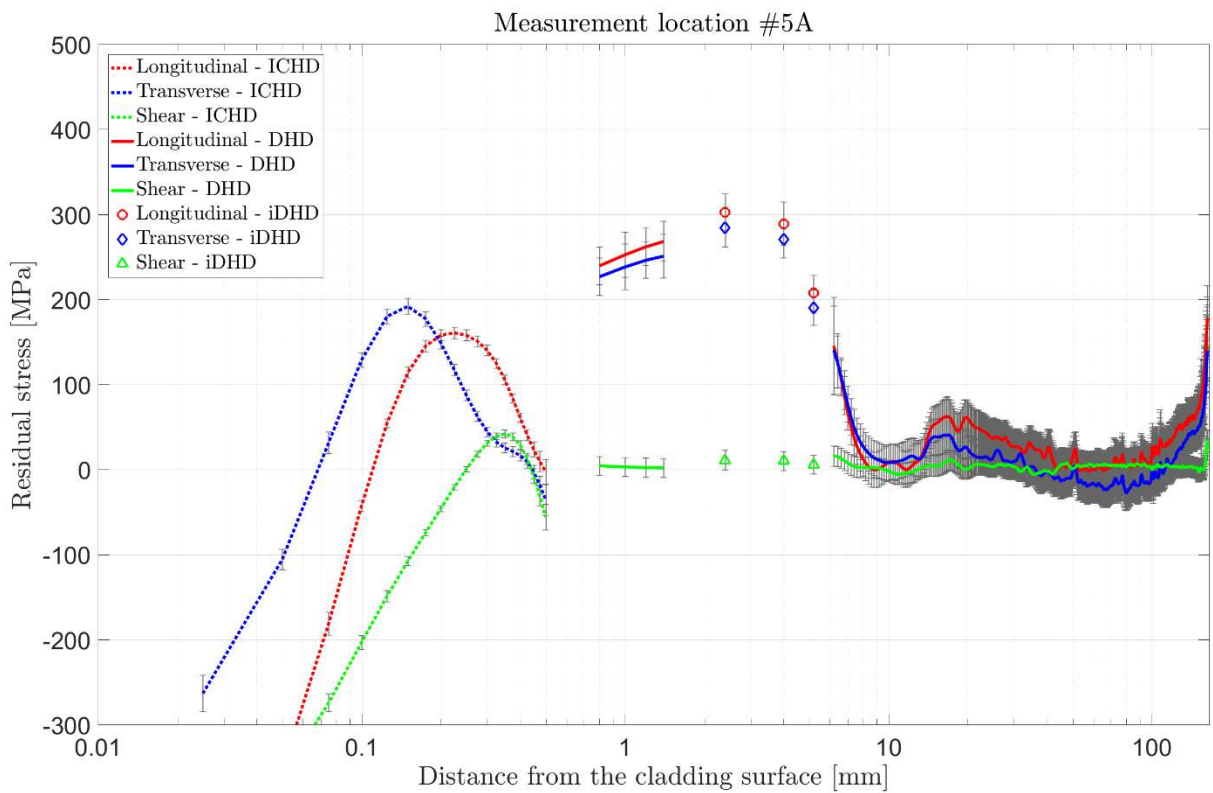


Figure 29 Residual stress measured by ICHD and iDHD/DHD at location #5A (mid-strip, at butt weld) after PWHT.

8. Discussion

The residual stress measurements by the iDHD/DHD technique seems to result in consistent measurement results from 1 mm depth and deeper. The results obtained by the ICHD technique is associated with a high sensitivity to small disturbances in the first and last 20% of the measurement depth, which is visible in the measurement results at depths smaller than 0.1 mm and for depths approaching 0.5 mm. The change in elastic modulus and mechanical properties near the clad to base metal interface may complicate the determination of residual strains and stresses.

The measured residual stresses were equi-biaxial throughout the thickness of the mock-up at all locations. The shear residual stresses were small compared with the transverse and longitudinal stresses.

In the as-welded cladding the measured residual stresses are very high (peak values in the range of 200 - 350 MPa), and also in the low-alloy ferritic base material with a peak value of about 425 MPa at a distance of approximately 8-12 mm from the cladding to low-alloy steel interface. The rapid changes in the stress distribution immediately beneath interface are assumed to be explained by solid state phase transformations (SSPT) in the low-alloy ferritic steel. As-welded residual stresses measured at the locations #3A (mid-strip) and #3B (mid-overlap) showed very similar distributions in terms of trend. Minimum and maximum peak values were observed at similar depths through the thickness, although the residual stresses within the base metal at location #3B are shifted approximately 5-10 mm relative those at location #3A.

The sudden drop in residual stresses immediately underneath the cladding is attributed to SSPT. SSPT results in changes in both volume and yield stress in situations where low-alloy steel is exposed to thermal cycling. The most significant displacive transformation takes place during cooling when austenite transforms into martensite [31]. Distortion of the crystal lattice gives rise to a misfit between regions that have transformed and regions that have not. This misfit gives rise to residual stresses and explains the localized compressive residual state [32]. The base metal microstructure undergoes a broad thermal excursion which may influence the yield characteristic stress.

Residual stress magnitudes in the cladding and the compressive zone in the low-alloy steel were significantly larger at the strip overlap location (#3B) compared to those at the mid strip location (#3A). This is likely explained by the fact that material in the overlap regions is subjected to an additional cycle of high strains and temperatures.

There is a clear balancing bending stress acting throughout the thickness of the base material after depositing the cladding. This stress distribution is related to the simply supported plate geometry and is expected to change for a cylindrical geometry.

The measurements after post weld heat treatment (PWHT) show that the residual stresses in the low-alloy base material (locations #7A and #7B) and its butt weld (location #5A) are substantially reduced. The tensile and balancing residual stresses in the ferritic base material and butt weld are reduced to levels below 75 MPa in the region for the as-welded peak values. For the cladding material, the heat treatment did not result in any significant stress relaxation. This can be expected since austenitic material is more heat resistant and the PWHT is designed for the low-alloy ferritic steel.

Cladding residual stresses after PWHT measured at the locations #7A (mid strip), #7B (strip overlap) and #5A (mid strip) show very similar distributions, with peak values at very similar depths. The residual stress magnitudes within the cladding at location #7B are higher than those at location #7A, which may be a result from the additional thermal cycling at strip overlap regions. The residual stresses in the cladding are influenced by the redistribution of the stress field in the base material during PWHT, and the residual stresses in the cladding were only slightly larger at location #7B compared to those at location #7A.

The measurements show slightly higher stresses in the cladding at location #5A. Due to the pre-existing ferritic butt weld, the thermal cycle during the cladding process serves as subsequent additional thermal cycling of the base material. It could be possible that the difference in the stress state in the base material before PWHT influences the relaxation in the ferritic steel and thus the final cladding stress state.

A compressive peak in the residual stresses is visible at about 30 mm depth in the measurements at locations #7A and #7B, but not at #5A (the butt weld in the low-alloy steel). There is no obvious explanation for this peak although it appears at a distance from the clad to base metal interface where the material is less affected by heat during welding.

The current results are compared to different previously performed measurements of residual stress and strain on strip clad blocks. The measurements on a 85 mm thick mock-up published in [7] indicate different results depending on the measurement method used. Measurements with the ring-core method in the as-welded and post weld heat treated conditions show high tensile residual stresses in the cladding up to 250-350 MPa. Measurements with the slitting/layering method indicate as-welded residual stresses up to 350-500 MPa in the low-alloy ferritic steel immediately beneath the heat affected zone. These results are in relatively good agreement with the current measurements. In [7] compressive residual stresses were found within the low-alloy steel heat affected zone. The current measurements show much lower compressive stresses.

The levels of cladding residual stress measured in [8] agree with the current results while the values in [9], [10] and [11] are lower. The compressive state in

the heat affected zone immediately underneath the cladding observed in [8] was greater than the current results and those in [10] and [11].

In [12] measurements on a 125 mm thick mock-up also showed different results depending on the measurement method. Measurements with the sectioning method indicated as-welded residual stresses of about 250 MPa in the low-alloy steel immediately beneath the heat affected zone. Measurements with the deep-hole drilling method show high tensile residual stresses in the cladding, up to 250-400 MPa in the post weld heat treated condition. This is in line with the current measurements. The deep-hole drilling measurements show that the stresses in the base material are substantially reduced during post weld heat treatment. The compressive residual stress state in the low-alloy steel heat affected zone after post weld heat treatment indicated by the deep-hole drilling method was not captured by the sectioning method. Two different welding processes were studied. A greater compressive residual stress state was indicated in the heat affected zone for electro-slag welding (-100 MPa) compared to submerged arc welding (-50 MPa), even after post weld heat treatment.

The measurements on a 40 mm thick mock-up in as-welded condition published in [13] using deep-hole drilling and neutron diffraction show similar general trends but significant differences in detail. The measurements indicate residual stresses up to 175 MPa in the cladding, approximately 175-275 MPa within the low-alloy heat affected zone and compressive stresses of -125 to -200 MPa. The tensile residual stress in the cladding is lower in comparison to other references but this may be explained by sequentially reducing the thickness from the as-welded 80 mm to 40 mm before measurements to allow neutron diffraction measurements.

The experimental results in the present work are in good agreement with those in the above summarised previous measurements. The general shape and characteristics of the residual stress profiles are similar in as-welded and post weld heat treated conditions although there are differences in magnitudes. These are likely attributed to differences in the mock-up configuration, welding method, materials, plate thickness as well as measurement techniques.

A source of uncertainty in measured cladding residual stresses is the modulus of elasticity, which is essential for the assessment of residual stresses based on measured strain release. The solidification texture in the cladding suggests that the elastic properties are anisotropic rather than isotropic. Different modulus of elasticity were stated in the previously performed measurements referenced above. Elastic moduli in the cladding plane as low as 168 GPa (as-welded) and 179 GPa (annealed) were observed in [16]. The effect from anisotropy was not considered for the current measurements.

The residual stresses in the cladding and the region just below is of greatest interest with respect to defects, degradation and assessments of safety margins against fracture. The residual stresses measured for this region is showed in detail

in Figure 30 and Figure 31, to a depth of 40 mm into the low-alloy ferritic steel. The figures show the longitudinal and transverse residual stresses measured by iDHD/DHD at all locations and without error bars for better visualization. Note that the distance is defined from the nominal interface between the cladding and base material, but after welding the fusion line is a few millimetres into the base material.

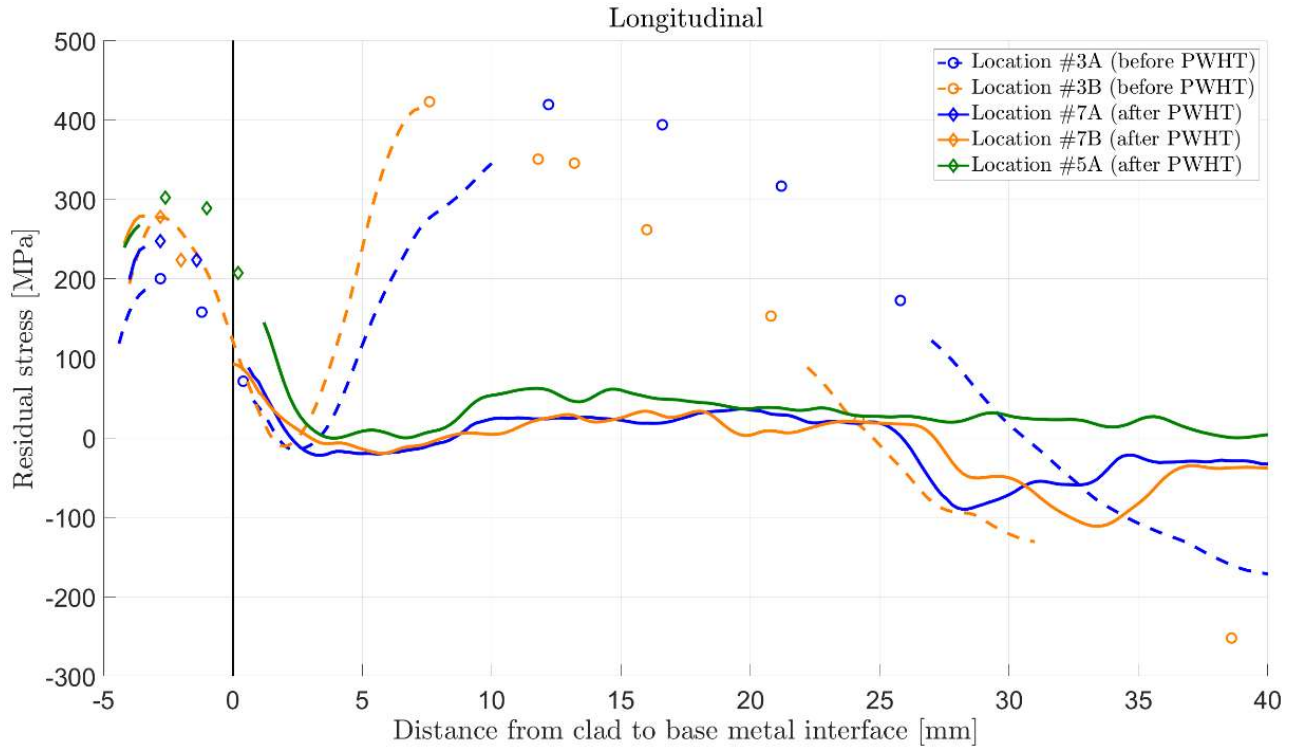


Figure 30 Longitudinal residual stress in the cladding mock-up measured by iDHD/DHD before and after PWHT. Location #3A and #7A are mid-strip, and #3B and #7B are mid-overlap.

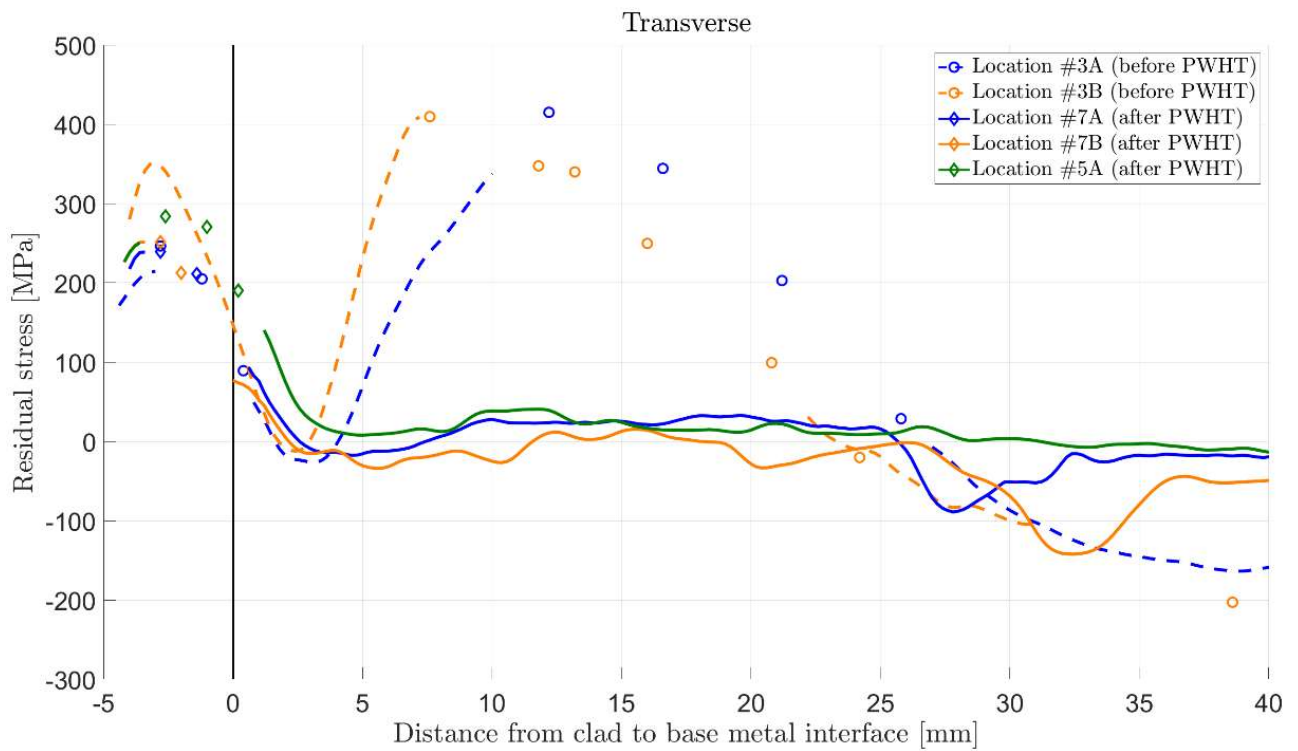


Figure 31 Transverse residual stress in the cladding mock-up measured by iDHD/DHD before and after PWHT. Location #3A and #7A are mid-strip, and #3B and #7B are mid-overlap

9. Conclusions

Weld residual stress and strain measurements were performed on a mock-up with single layer strip cladding common in reactor pressure vessels. The measurements were made on a mock-up consisting of a 160 mm thick low-alloy ferritic steel plate of type SA-508 Class 3 with a single layer weld deposited strip cladding of austenitic stainless steel E308L. The cladding was manufactured with submerged arc strip welding adapted to a procedure used for reactor pressure vessels in the 1970s.

During manufacturing comprehensive measurements of the thermal response at the welding was recorded to provide information for validation of numerical modelling. Detailed through-thickness measurements of residual stresses were performed using the methods deep-hole drilling and incremental centre-hole drilling. Measurements were performed at two different locations in the as-welded state and at three different locations after post weld heat treatment.

The measurements show that high tensile residual stresses are found in the clad material and about 30 mm into the low-alloy ferritic steel after welding. The residual stresses in the clad layer and in the steel plate are in the order of the yield stress in each material. The measurements show that the residual stress distribution through the clad block is equi-biaxial. Further, measurements after post weld heat treatment (PWHT) show that the residual stresses in the low-alloy ferritic base material and butt weld were substantially reduced, whereas no significant reduction was observed for the residual stresses in the stainless steel cladding.

The residual stress measurements were carried out through the thickness at five various locations. Measurements at locations #3A and #3B were performed as-welded whereas the measurements at locations #7A, #7B and #5A were performed after post weld heat treatment (PWHT). The measured residual stresses are summarized for the as-welded state and after PWHT.

As-welded:

- Transverse and longitudinal residual stresses are in general very similar and the shear component is negligible, the stress state is close to equi-biaxial. There is some difference in residual stress magnitudes and trend between the mid strip (#3A) and strip overlap (#3B) regions.
- Residual stresses within the cladding reach maxima between 200 MPa and 245 MPa at location #3A and between 275 MPa and 350 MPa at location #3B. The measurements at location #3B show higher residual stress and with a larger difference between the transverse and longitudinal components. The differences may be connected to the additional thermal cycling at strip overlap regions. The mid strip locations have experienced one thermal cycle whereas the strip overlap locations have experienced two thermal cycles. It is not unlikely that the cladding at the measurement

location is partially or even completely remolten down to the base metal during the second thermal cycling, while the base metal is subjected to a second major thermal cycle.

- Residual stresses within the low-alloy ferritic base metal reach maxima between 410 MPa and 425 MPa approximately 8-12 mm below the dissimilar metal interface between the cladding and base material. The residual stresses drops to a compressive state with minima between -250 MPa and -165 MPa at a depth of approximately 45 mm.
- There is a sudden drop in residual stresses immediately underneath the cladding which is attributed to solid state phase transformations.
- The block was cladded without any external restraint and this boundary condition results in a longitudinal and transverse distortion due to shrinkage in the as-welded state. This results in a balancing bending component in the base metal notable from 40 mm depth and through the remainder of the thickness.

After PWHT:

- Transverse and longitudinal residual stresses are very similar and the shear component is negligible. There is a small difference in residual stress magnitudes and trend between the mid strip (#7A) and strip overlap (#7B) regions. An additional measurement (#5A) was undertaken mid strip directly above a post weld heat treated pre-existing low-alloy butt weld.
- Residual stresses within the cladding reach maxima between 240 MPa and 300 MPa. This confirms a limited relaxation within the cladding, which is expected at these PWHT temperatures. The residual stress magnitudes within the cladding at location #7B are slightly higher than those at location #7A. The residual stresses in location #5A is the highest which may be a result from the additional thermal in the base material.
- Residual stresses within the low-alloy ferritic base metal were substantially relaxed during PWHT. The initial maxima present in the as-welded state have been relaxed to levels below 75 MPa. This corresponds to a reduction of maximum values to about 80 percent.
- The significant bending component observed in the as-welded state vanished almost completely as a result from PWHT. Remaining is a fairly constant and small compressive state through most of the base metal.

The experimental results in the present work agree with those in previously performed measurements. The general shape and characteristics of the residual stress profiles are similar in many cases and there are differences in magnitudes. These differences may be attributed to differences in the mock-up configuration, welding method, materials, plate thickness as well as measurement techniques.

Another source of uncertainty in measured cladding residual stresses is the modulus of elasticity, which was not considered for the current measurements.

The high stresses in the low-alloy ferritic steel in the as-welded condition may possibly contribute to explain why under-clad cracks sometimes occur during manufacturing. Note however that the high stresses occur in the region 5-25 mm below the clad to base metal interface in this case.

Generally somewhat higher stress levels were measured in the cladding at mid-overlap locations compared to mid-strip locations.

After PWHT the residual stresses are substantially reduced in the low-alloy ferritic steel, down to about 75 MPa, emphasising the importance of documenting the PWHT performed.

Neutron embrittlement of the reactor pressure vessel generally limits the possible long-term operation of a nuclear power plant to e.g. 60 or 80 years. Sufficient remaining safety margins with respect to fracture has to be verified by structural integrity analyses that consider the plant surveillance tests results, defects in and near the cladding, the dimensioning load cases, and also residual stresses in the reactor pressure vessel. For these reasons good understanding and well documented estimates of the residual stresses in the cladding are very valuable.

The residual stresses measured in the mock-up deviates from the residual stresses in a clad reactor pressure vessel, since the mock-up was not subjected to pressure test. However, the detailed results presented in this report are very valuable for validation of numerical modelling, which can be used to predict the residual stress state including effects of pressure tests and operational loads, for cylindrical geometries, and for cladding processes other than submerged arc strip welding.

10. Contribution statement

Ringhals AB contributed with the low-alloy base metal, thermal response measurements and has been an important discussion partner throughout the project.

ESAB contributed with preparation, instrumentation, cladding materials and overlay welding at their facilities in Sweden.

Weld residual stress measurements; before heat treatment at locations #3A, #3B and #3C were financed by the Swedish Radiation Safety Authority, after heat treatment at locations #7A, #7B and #7C were financed by Forsmarks Kraftgrupp AB, after heat treatment at location #5A were financed by Ringhals AB.

The welding residual stress measurements were performed and documented by Veqter Ltd. at their facilities in UK. Veqter coordinated the post weld heat treatment performed at Thermofax in UK.

Kiwa Technical Consulting AB devised the project, performed the overall planning, direction and coordination of all details, and wrote the final report. The sections of the report directly related to the weld residual stress measurements are based on the documentation provided by Veqter.

The Swedish Radiation Safety Authority, Ringhals AB and Forsmarks Kraftgrupp AB have reviewed the final report.

11. Acknowledgement

This work was supported by the Swedish Radiation Safety Authority, Ringhals AB, Forsmarks Kraftgrupp AB and ESAB.

All support received during this project is gratefully acknowledged.

12. References

- [1] M. Patel, R. Madnani, B. Chauhan and S. Sundaresan, "Application of electrosag strip cladding for reactors in hydrogen-based refinery service," 2009.
- [2] H. Gripenberg, H. Keinänen, C. Ohms, H. Hänninen, D. Stefanescu, D. J. Smith, "Prediction and Measurement of Residual Stresses in Cladded Steel," *Materials Science Forum*, pp. 861-866, 2002.
- [3] G. Reddy and D. Ayres, "High-temperature elastic-plastic and creep properties for SA533 Grade B Class I and SA508 materials," Combustion Engineering, Inc., Windsor, CT (USA), 1982.
- [4] "Practical Guidelines for the Fabrication of High Performance Austenitic Stainless Steels," Nickel Institute and International Molybdenum Association (IMOA), 2010.
- [5] D. A. Canonico, "Significance of Reheat Cracks to the Integrity of Pressure Vessels for Light-Water Reactors," NUREG-15, 1977.
- [6] W. Bamford and R.D. Rishel, "A Review of Cracking Associated with Weld Deposited Cladding in Operating PWR Plants," WCAP-15338-A, 2002.
- [7] P. Dupas and D. Moinereau, "Evaluation of Cladding Residual Stresses in Clad Blocks by Measurements and Numerical Simulation," *Journal De Physique IV*, vol. 6, 1996.
- [8] D.P. Jones; W.R. Mabe; J.R. Shadley; E.F. Rybicki, "WAPD-T-3181: Residual stresses in weld deposited clad pressure vessels and nozzles," 1998.
- [9] T.L. Dickson; W.J. McAfee; W.E. Pennell; P.T. Williams, "Evaluation of Margins in the ASME Rules for Defining the P-T Curve for a RPV," Oak Ridge National Laboratory, 1998.
- [10] G. Neber; A. Roth, "Residual stress measurement on the RPV head of Ringhals 2 NPP- Summary Report," Report No. SNP NT1/2000/E356a, Framatome ANP, 2001.
- [11] NESC-IV Project, "An investigation of the transferability of master curve technology to shallow flaws reactor pressure vessel application," NESC-IV Report No. 4 (05), JRC, European Commission, 2005.
- [12] J. Katsuyama, H. Nishikawa, M. Udagawa, M. Nakamura and K. Onizawa, "PVP2010-25541: Assessments of Residual Stress Due to Weld-Overlay Cladding and Structural Integrity of Reactor Pressure Vessel," in *Proceedings of the ASME 2010 Pressure Vessels & Piping Division*, Bellevue, Washington, USA, 2010.
- [13] M. James, M. Newby, P. Doubell, D. Hattingh, K. Serasli and D. Smith, "Weld residual stresses near the bimetallic interface in clad RPV steel: A comparison between deep-hole drilling and neutron diffraction data," *Nuclear Engineering and Design*, vol. 274, pp. 56-65, 2014.
- [14] ASME, "Boiler & Pressure Vessel Code Section II - Materials - Part D - Properties (Metric)," 2011.
- [15] Metals Handbook, Properties and Selection: Irons, Steels and High, tenth ed., vol. 1, ASM International, 1990.
- [16] W. Vandermeulen, M. Scibetta, A. Leenaers, J. Schuurmans and R. Gérard, "Measurement of the Young modulus anisotropy of a reactor pressure vessel cladding," *Journal of Nuclear Materials*, vol. 372, pp. 249-255, 2008.

- [17] ESAB, “Technical Handbook - Strip cladding - Fluxes and strips for submerged arc and electroslag strip cladding”.
- [18] Metrode Welding, Consumables Strip Cladding Applications - Rev 04, 2012.
- [19] N. Thalberg and B. Gustafson, “Welding procedure specification - SA-38-44,” 1977.
- [20] Thermofax Ltd, “Heat Treatment Chart Data - Batch No 24670 - Heat No 18486”.
- [21] E. Kingston, D. Stefanescu, A. Mahmoudi, C. Truman and D. Smith, “Novel Applications of the Deep-Hole Drilling Technique for Measuring Through-Thickness Residual Stress Distributions,” *Journal of ASTM International*, vol. 3, no. 4, pp. 1-12, 2006.
- [22] A.H. Mahmoudi et al, “A New Procedure to Measure Near Yield Residual Stresses Using the Deep Hole Drilling Technique,” *Experimental Mechanics*, vol. 49, pp. 595-604, 2009.
- [23] A. Garcia-Granada, D. George and D. Smith, “Assessment of Distortions in the Deep Hole Technique for Measuring Residual Stresses,” in *Proceedings of the 11th International Conference on Experimental Mechanics*, Oxford, 1998.
- [24] D. Goudar, C. Truman and D. Smith, “Evaluating Uncertainty in Residual Stress Measured Using the Deep-Hole Drilling Technique,” *Strain*, vol. 47, pp. 62-74, 2009.
- [25] D. George, E. Kingston and D. Smith, “Measurement of through-thickness stresses using small holes,” *The Journal of Strain Analysis for Engineering Design*, vol. 37, no. 2, pp. 125-139, 2002.
- [26] ASTM-E837-13a, “Standard Test Method for Determining Residual Stresses by the Hole-Drilling Strain Gage Method,” ASTM, 2013.
- [27] P. Grant, J. Lord and P. Whitehead, “The measurement of residual stresses by the incremental hole drilling technique,” *Measurement Good Practice Guide*, no. 53, 2006.
- [28] A. Ajovalasit, G. Petrucci and B. Zuccarello, “Determination of Nonuniform Residual Stresses Using the Ring-Core Method,” *Journal of Engineering Materials and Technology*, vol. 118, pp. 224-228, 1996.
- [29] B. Zuccarello, “Optimization of depth increment distribution in the ring-core method,” *Journal of Strain Analysis for Engineering Design*, vol. 31, no. 4, pp. 251-258, 1996.
- [30] K. Serasli, “Residual stress measurements through a clad block. Report No.: R15-021,” Veqter Ltd., 2017.
- [31] A.H. Yaghi, T.H. Hyde, A.A. Becker and W. Sun, “Finite element simulation of welding and residual stresses in a P91 steel pipe incorporating solid-state phase transformation and post-weld heat treatment,” *The Journal of Strain Analysis for Engineering Design*, vol. 221, pp. 213-224, 2008.
- [32] P.J. Withers, “Residual stress and its role in failure,” *Reports on Progress in Physics*, pp. 2211-2264, 2007.

The Swedish Radiation Safety Authority has a comprehensive responsibility to ensure that society is safe from the effects of radiation. The Authority works from the effects of radiation. The Authority works to achieve radiation safety in a number of areas: nuclear power, medical care as well as commercial products and services. The Authority also works to achieve protection from natural radiation and to increase the level of radiation safety internationally.

The Swedish Radiation Safety Authority works proactively and preventively to protect people and the environment from the harmful effects of radiation, now and in the future. The Authority issues regulations and supervises compliance, while also supporting research, providing training and information, and issuing advice. Often, activities involving radiation require licences issued by the Authority. The Swedish Radiation Safety Authority maintains emergency preparedness around the clock with the aim of limiting the aftermath of radiation accidents and the unintentional spreading of radioactive substances. The Authority participates in international co-operation in order to promote radiation safety and finances projects aiming to raise the level of radiation safety in certain Eastern European countries.

The Authority reports to the Ministry of the Environment and has around 300 employees with competencies in the fields of engineering, natural and behavioral sciences, law, economics and communications. We have received quality, environmental and working environment certification.

Publikationer utgivna av Strålsäkerhetsmyndigheten kan laddas ned via stralsakerhetsmyndigheten.se eller beställas genom att skicka e-post till registrator@ssm.se om du vill ha broschyren i alternativt format, som punktskrift eller daisy.

Strålsäkerhetsmyndigheten
Swedish Radiation Safety Authority
SE-171 16 Stockholm
Phone: 08-799 40 00
Web: ssm.se
E-mail: registrator@ssm.se

©Strålsäkerhetsmyndigheten